DESIGN OF PHOTOREGULATED RIBONUCLEASE

by

Y. David Liu

A thesis submitted in conformity with the requirements

for the degree of Master of Science

Graduate Department of Chemistry

University of Toronto

God grant me the Serenity to accept the things I cannot change...Courage to change the things I can and Wisdom to know the difference.

------- From Bible

This thesis is dedicated to my father Ruhan Liu and my mother Guanglan Liu for their great love and support throught the duration of this work.

ACKNOWLEDGEMENT

I express my deepest gratitude to my supervisor Professor G. A. Woolley for his enthusiasm, great supervision and support in many ways during my study in his lab. He is very knowledgeable, and also his understanding made me feel happy working in his lab. In particular, his helpful support made this project to be complete successfully. I have learned a lot from him not only in the chemistry and biochemistry field, but also in doing research and learning the English language. He encourages me in many ways. All of these made my stay at the University of Toronto very memorable.

I would like to thank Professor A. M. MacMillan for reading, and John Karanicolas for molecular modelling and figures and all the staff and students in my lab for their help.

Financial assistance from the University of Toronto, in terms of teaching assistantships and research assistantships, is greatly appreciated.

A very special thanks to my wife Renee Ren for her love, my Australian friend Mr. John Koorey and his family and my Canadian friend Mr. Wayne Hamilton and his family for their tremendous support and faith in me.

ABSTRACT

DESIGN OF PHOTOREGULATED RIBONUCLEASE

by

Y. David Liu

Master of Science

Graduate Department of Chemistry

University of Toronto, 1997

Bovine pancreatic ribonuclease A (RNAse A) is a well defined enzyme that has been used as a test protein in the study of a wide variety of chemical and physical methods applied to protein chemistry. The design of a photoregulated RNAse is a test case for rational design of a photoregulated enzyme. If one could design photoregulated biomolecules, then a variety of cellular processes could be studied using light as a tool.

A photoisomerizable amino acid residue phenylazo-phenylalanine (PAP) was synthesized and incorporated into S-peptide analogues using solid phase peptide synthesis techniques. Noncovalent reassociation of S-peptide analogues bearing PAP residues at positions 4, 8 and 11 with S-protein was examined. PAP-4 and PAP-11 analogues were able to reconstitute ribonuclease activity. Photoisomerization of the PAP-4 peptide modulated enzyme activity.

TABLE OF CONTENTS

INTRODUCTION

A. Photochemical Switches

Photosensitive systems play an important role in Nature because several important biological processes are triggered by light signals and controlled by the nature of the light source (1). All these systems have a common feature that chromophores or "photoreceptors" are incorporated in the system and interact in specific ways with the biological environment. If one could design photoregulated biomolecules, then a variety of cellular processes could be studied using light as a tool.

Two different types of photoswitches can be identified (1):

1) Single-cycle photoswitch: A photosensitive group is bound to the biomaterial. The biological activity of the complex is blocked when the group is attached. Light causes release of the photosensitive group. This activates the biomaterial (3, 4) (Figure 1).

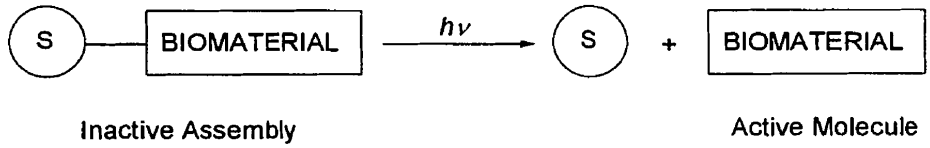

Figure 1 Design of a single-cycle photobiological switch S = photosensitive group

2) Multicycle photobiological switch. Light of one wavelength switches the biomaterial to an active form. The complex converts to an inactive form when light of a second wavelength is applied. The reverse reaction may occur through a different pathway (e.g. thermal isomerization) (Figure 2).

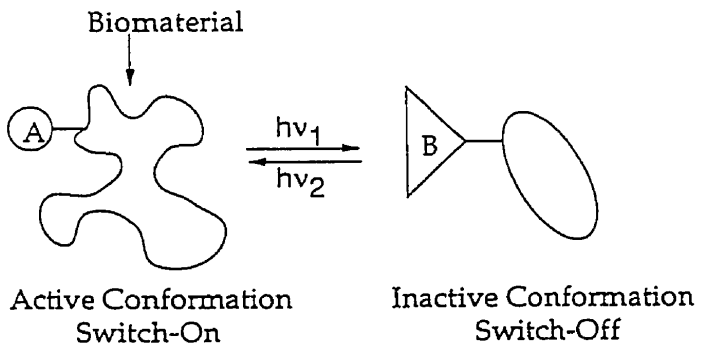

Figure 2 Design of a multicycle photobiological switch (1)

Reversible photoregulation can also be divided into two types:

(i) Photoregulation by small molecule binding

An inhibitor or cofactor binds to the protein's active site in one photoisomeric state as a low molecular-weight deactivator or activator of protein. The low molecular-weight component is released from the protein active site in the complementary photoisomeric state (2, 5 - 11). In this way, a photoisomerizable inhibitor or cofactor with only one state recognizable by the biomaterial could reversibly switch on and off its biological functions (Figure 3)

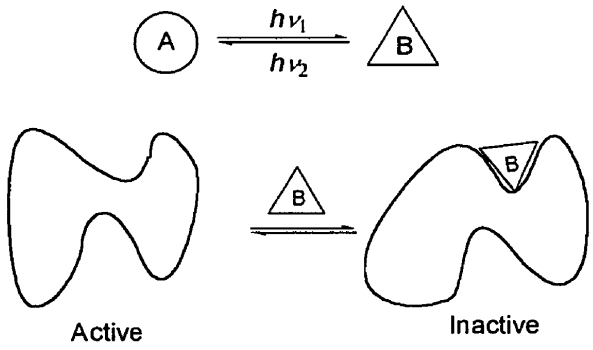

Figure 3 Reversible photoregulation of biomaterial by small molecule binding

(ii) Photochemical control via covalently-linked chromophores

Isomerization of covalently-linked photosensors can alter biomolecule structure and activity. For example, azobenzene-modified poly (L-glutamic acid) (12, 13) undergoes photoregulation of structure in the presence of appropriate surfactants. Trans-azobenzene-poly (L-glutamic acid) (**1a**) isomerizes to cis isomer (**1b**) at 370 nm, and cis isomer (**1b**) reisomerizes back to trans isomer (**1a**) upon illumination at 450 nm. Photoisomerization causes changes in the pK_a values of the glutamate residues which depend on the isomeric structures of the azobenzene units (pK_a = 6.8 for **1a** and 6.3 for **1b**). It has been suggested that the polarity of cis-azobenzene units enhances the local dielectric constant of neighbouring carboxylic acid functionalities and thus causes the difference in the pK_a (14). Photoisomerization thus affects the

protonation state, and, in turn, the structure of the polymer changes from coil to helix.

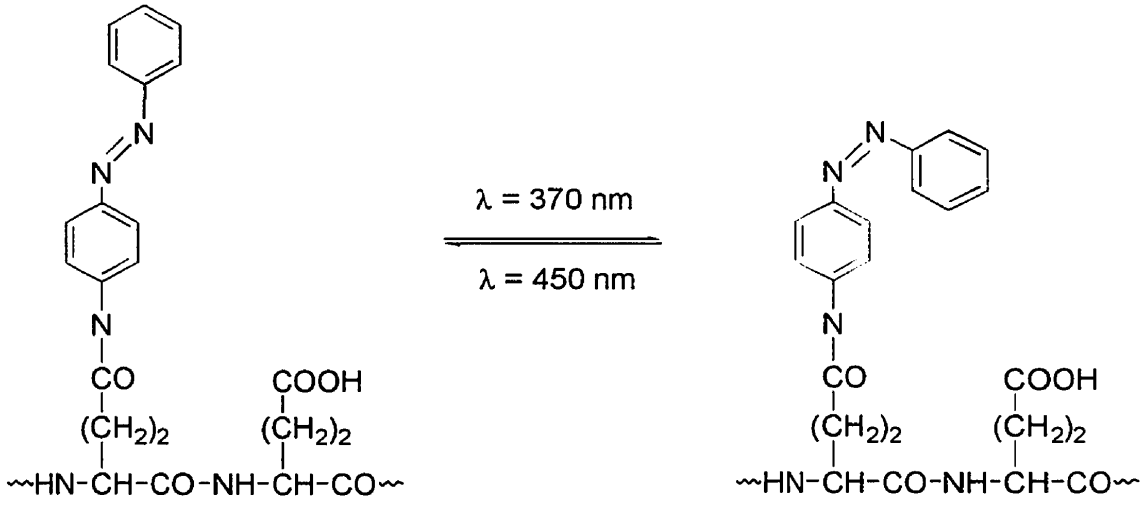

1a **1b**

B. Photoregulation of Enzymes

Photocontrol of enzyme activity can allow one to study cellular biochemistry by using light. Photocontrol may be either reversible or irreversible.

(i) Irreversible regulation

An example of irreversible regulation of enzyme activity is the removal of a caging group from an enzyme used to control protein splicing (15).

Protein splicing is a post-translational rearrangement process (15). It produces two proteins (excised intein and ligated exteins) from a single precursor (Figure 4)(16, 17).

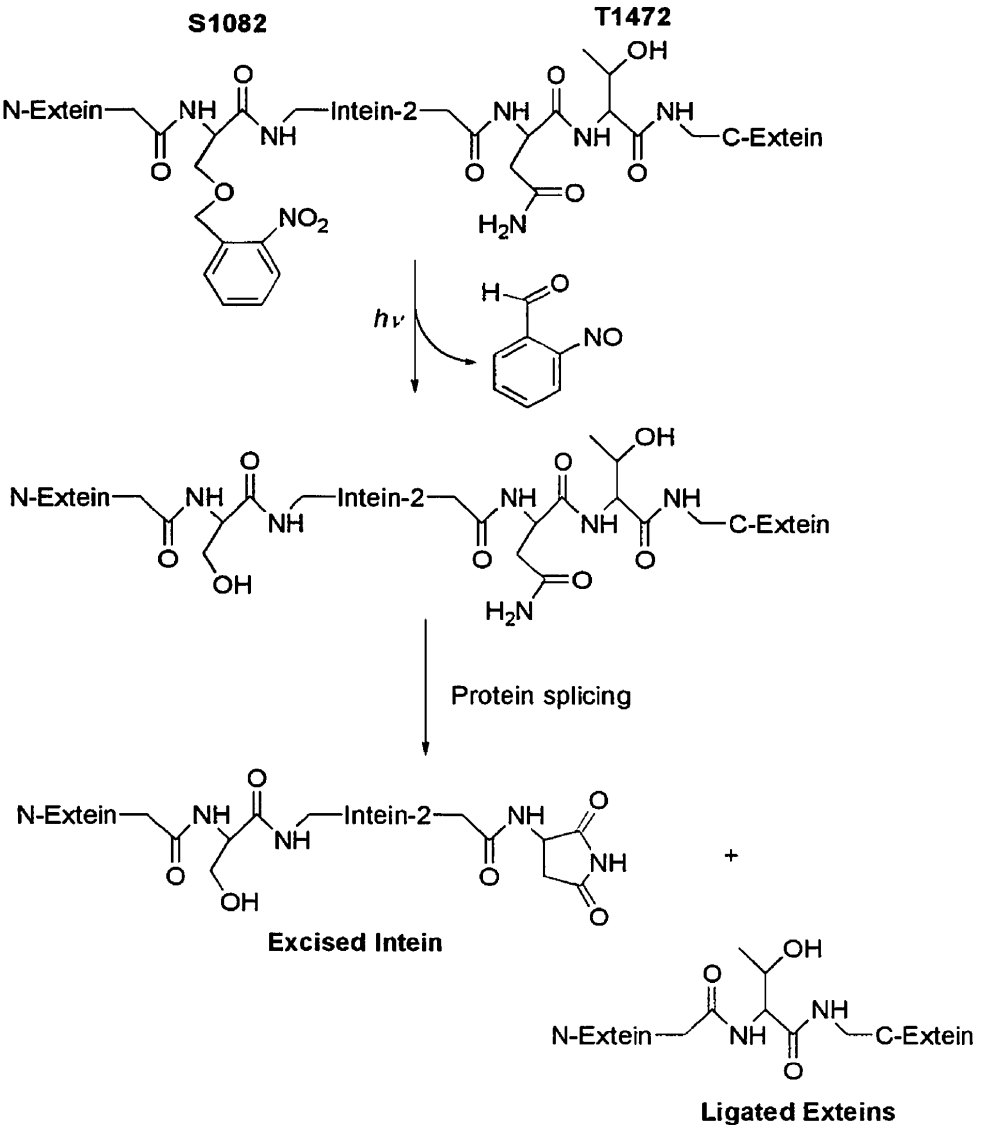

Figure 4 Initiation of protein splicing of truncated *Thermococcus litoralis* DNA polymerase by photolysis of 2-nitrobenzyl ether at the upstream splice junction (17).

The DNA polymerase of *Thermococcus litoralis* has a Ser1082 at the upstream splice junction and a Thr1472 at the downstream junction. A "caged" protein was prepared by incorporation of O-(2-nitrobenzyl) serine *in vitro* through suppression of the corresponding amber nonsense mutation with chemically aminoacylated supressor tRNA (18). The caged protein converts to the wild-type upon irradiation at 300-350 nm, which removes the 2-nitrobenzyl group and splicing process occurs normally (19).

A particularly successful example of enzyme photoregulation has been reported by Creighton and Bender (20, 21) with serine proteinases. Serine proteinases have been used as target enzymes for the development of photoregulation because they are widespread in nature and their catalytic mechanism is well understood. Serine proteinases catalyze hydrolysis of peptide bonds. In the mechanism of serine proteinase action, Ser195 carries out a nucleophilic attack on substrate. The imidazole ring of His57 takes up the proton during the formation of the tetrahedral intermediate. The tetrahedral intermediate decomposes to an acylenzyme intermediate. Hydrolysis of the acylenzyme intermediate regenerates active enzyme (Figure 5) (22).

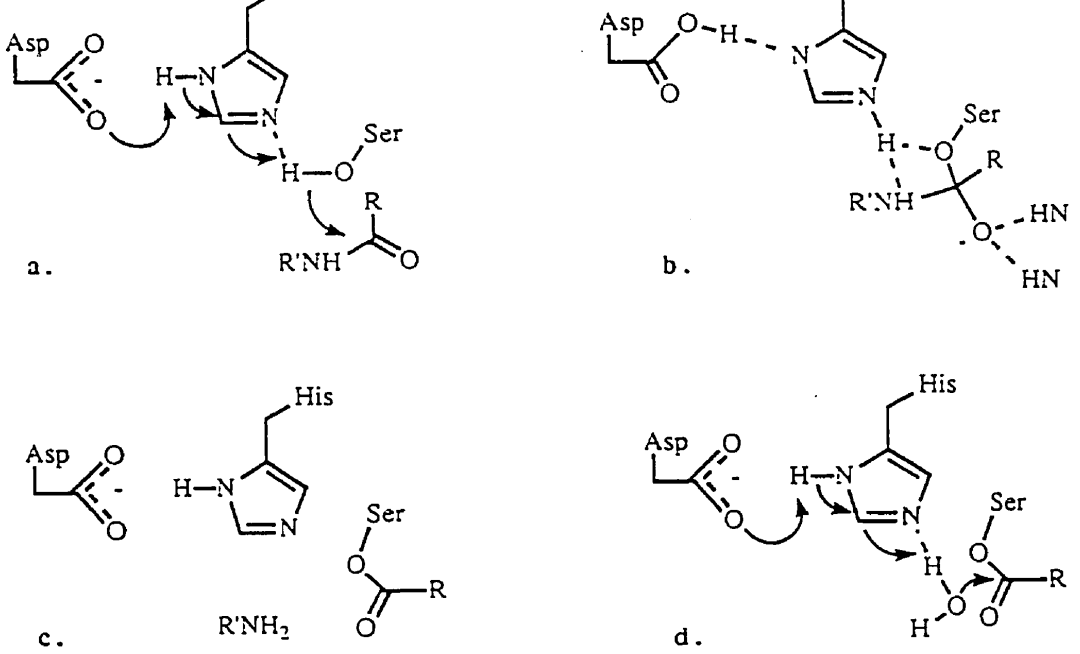

Figure 5 Mechanism of serine proteinase action: (a) active form of the enzyme; (b) tetrahedral intermediate; (c) acylenzyme intermediate; (d) enzyme deacylation (22)

Turner (1987) and his co-workers (23, 24) discovered o-hydroxycinnamates efficiently acylate the active site serine of serine proteinase to form acylenzymes. The acylenzymes are inactive and very stable in the absence of light. Photoisomerization of the acylenzymes leads to rapid enzyme deacylation by intramolecular lactonization. Thus, irradiation removes cinnamates and regenerates the active enzymes. This mechanism of photoactivation of serine proteinases is shown below (Figure 6).

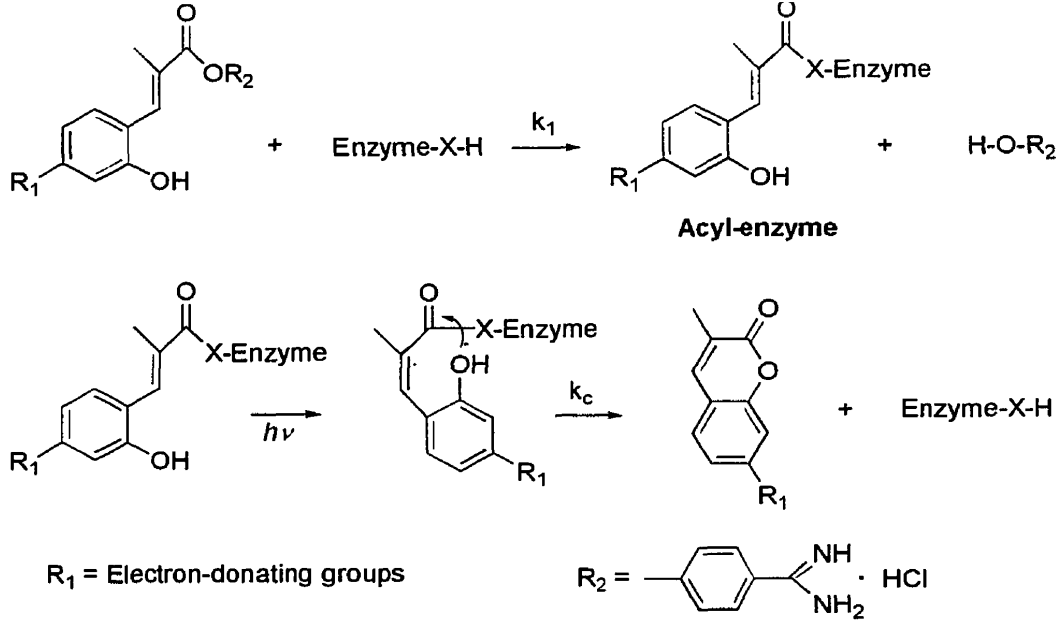

Figure 6 Photoactivation of serine proteinases (24): The o-hydroxycinnamate inhibitor reacts with enzyme active site Ser-OH group and forms trans-acylenzyme (inactive). The trans-acylenzyme converts to cis-acylenzyme after irradiation. This is followed by rapid enzyme deacylation (intramolecular cyclization) which regenerates the active enzyme.

The o-hydroxycinnamate inhibitors must meet 3 requirements necessary for effective photoactivation: 1) The trans-acylenzyme must be stable in the dark and its hydrolysis must be very slow in order that it can be controlled by photoisomerization (Figure 7).

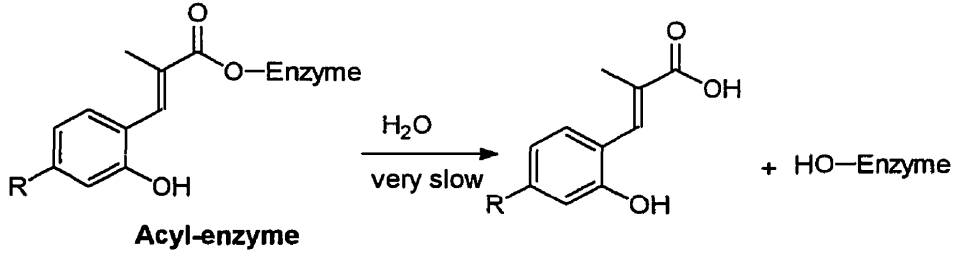

Figure 7 Hydrolysis of trans acylenzyme

Electronic effects influence the stability of trans-acylenzyme. The rate of deacylation is slowest when electron-donating groups are present on para position (R) of the cinnamate aromatic ring (Figure 7). Electron-donating groups directly conjugate with the acyl group and stablize the acylenzyme. 2) Trans to cis photoisomerization should be fast, occur efficiently and require moderate light intensities. 3) The rate of hydrolysis of cis-acylenzyme must be fast. Once photoisomerization occurs, the cis-acylenzyme lactonizes very rapidly through a tetrahedral intermediate. The catalytic residues in the enzyme active site promote lactonization as acid or base catalysts.

(ii) Reversible regulation by small molecule binding

As described above, one strategy for photoregulation is to alter a small effector molecule with light, and as a result, enzyme activity is altered Photoisomerizable inhibitors can photoregulate enzymes by using trans-cis photoisomerization of azobenzene compounds (5, 6). N-p-phenylazophenyl trimethylammonium chloride (**2a, 2b**) and N-p-

phenylazophenyl carbamoylcholine iodide (**3a, 3b**) are competitive inhibitors toward the enzyme acetylcholinesterase.

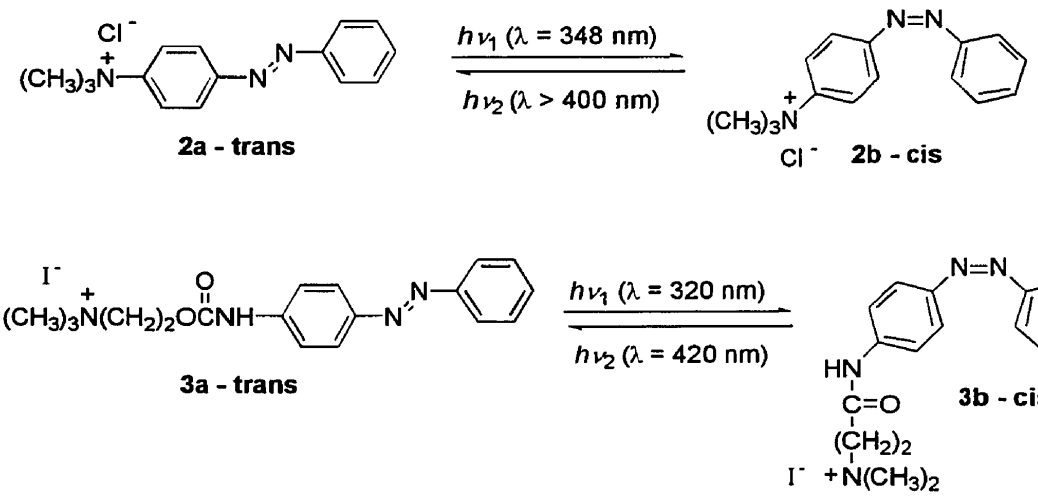

The inhibition constants of trans and cis isomers are different. For example, the inhibition constants of 2a-trans and 2b-cis are 1.6 mM and 3.6 mM, respectively (5, 6). The difference is 2.0 mM, and this difference of inhibition constants of trans-cis isomers is sufficient to photoregulate the activity of acetylcholinesterase by changing the effective inhibitor concentration.

(iii) Reversible regulation via covalently attached chromophores

The alternative strategy of photoregulation (via covalently attached units) has also been demonstrated with enzymes. For instance, trans-4-

carboxyazobenzene (**4**), trans-3-carboxyazobenzene (**5**) and trans-2-carboxyazobenzene (**6**) have been linked to lysine residues in the enzyme papain by covalent coupling. This then modifies the enzymatic activity of papain by reversible trans ↔ cis photoisomerization of the azobenzene component (25).

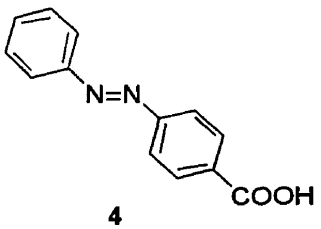

4

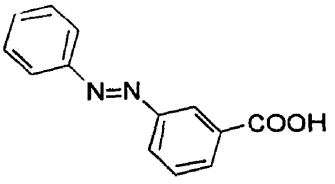

5

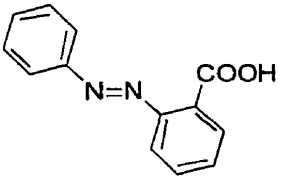

6

(Trans-4-carboxyazobenzene)-papain, (trans-3-carboxyazobenzene)-papain, and (trans-2-carboxyazobenzene)-papain keep 80%, 36% and 1% of the activity of the native enzyme, respectively. The photoregulation studies indicated that the 4-carboxyazobenzene-papain complex (**7**) showed the best photostimulated activity.

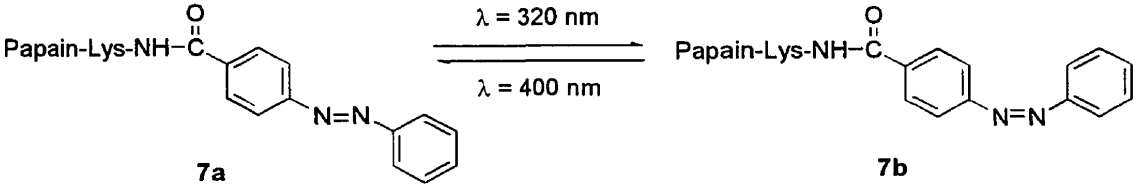

7a **7b**

Another example is a photoisomerizable mutant of phospholipase A_2 (26, 27). The enzyme cleaves 2-acyl bonds of phosphoglycerides, and it is more active to substrates which are associated with aggregated interfaces (micelles or vesicles) than substrates with non-aggregated interfaces. The enzyme recognition site at the interface adopts an α-helical conformation which helps association of the enzyme at the lipid-water interfaces (28). A photoisomerizable phospholipase A_2 mutant was prepared by semisynthesis (29). The Trp3 residue was replaced with the photoisomerizable residue phenylazophenylalanine (PAP). The trans-PAP mutant did not show any lipid hydrolysis activity. The cis-PAP mutant, however, showed enhanced lipid hydrolysis. The α-helix content of cis-mutant was also much higher than that of trans-mutant (28). It was suggested that the enzyme is deactivated due to the perturbation of the recognition site interface in the trans-mutant. Once the photoisomerization to cis-mutant occurs, the recognition site is reconstituted and the enzyme activity is switched on (28).

The work by Ueda et al., with phospholipase A2 is the only published example of reversible photocontrol of enzyme activity in which some knowledge of the three-dimensional structure of the enzyme was used to direct the design of photoregulation. Other examples (e.g. papain above) simply employed non-specific enzyme modification by photoisomerizable groups. To optimize the extent of photoswitching, it will be necessary to

have information on the structural consequences of photoisomerization. Rational design of photoswitching would be facilitated if photochromic groups could be incorporated site-specifically at key sites in the enzyme structure. For instance if enzyme activity is to be modulated by interfering with substrate access to the active site, close control of the positioning of photosensitive groups will be necessary. For these reasons we chose to employ a structurally well-defined enzyme as a target for developing methods of enzyme photoregulation.

C. Ribonuclease A

Bovine pancreatic ribonuclease A (Mr 13680) is a single polypeptide sequence of 124 amino acid residues and four disulphide bonds (30). It is a well charaterized enzyme with a structure defined to high resolution by X-ray crystallographic methods (31, 32). It has been used a test protein for the application of a wide variety of chemical and physical methods to protein chemistry (33, 34).

Ribonuclease A catalyses the hydrolysis of single stranded RNA at the 5'-O-P ester bond in a two-step process (Figure 8) (35). The first step yields a 2', 3'-cyclic phosphate terminus and a free 5'-OH group. The subsequent hydrolysis of the cyclic phosphate is usually much slower

(36). The base at the 3'-side of the bond cleaved must be a pyrimidine - uracil or cytosine.

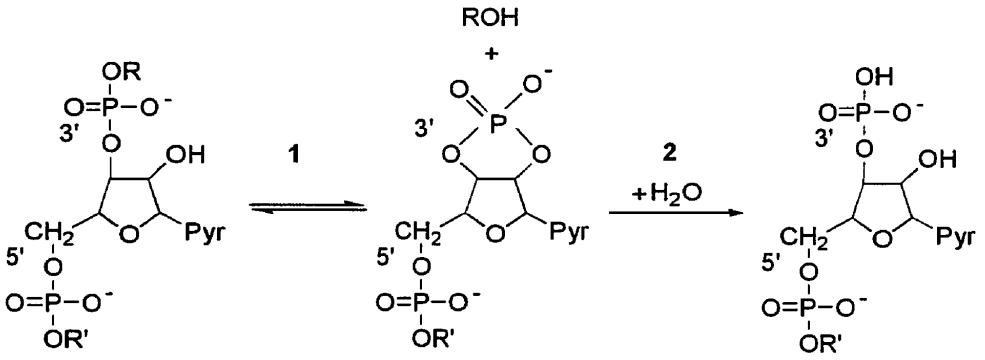

Figure 8 The two-step hydrolysis of RNA (36)

The detailed chemical mechanism of ribonuclease is still debated (37). In particular, it is not clear if the transition state leading to the cyclic intermediate is like a diionic phosphorane or a monoionic phosphorane/triester. It is clear, however, that key residues in the ribonuclease A active site contribute to catalysis via both Bronsted acid and Bronsted base catalysis.

A plot of the activity of ribonuclease A versus pH is bell-shaped with a maximum activity near neutrality (35). The activities of many enzymes vary with pH. This is because the active sites generally contain important acidic or basic groups (Table 1).

Table 1. pKa's of ionizing groups

Group	pKa	
	Model compounds (small peptides)	Usual range in proteins
Amino acid a-CO2H	3.6	
Asp (CO2H)	4.0	2-5.5
Glu (CO2H)	4.5	
His (imidazole)	6.4	5-8
Amino acid a-NH2	7.8	~8
Lys (-NH2)	10.4	~10
Arg (guanidine)	~12	—
Tyr (OH)	9.7	9-12
Cys (SH)	9.1	8-11
Phosphates	1.3, 6.5	—

a. Data mainly from C Tanford, *Adv. Protein Chem.* **17**, 69 (1962); C Tanford and R. Roxby, Biochemistry **11**, 2192 (1972); Z. Shaked, R. P. Szajewski, and G. M. Whitesides, *Biochemistry* **19**, 4156 (1980) (38)

The pH dependence of ribonuclease A is attributed to the ionizations of two active site histidine residues - His119 and His12 (34). The pH dependence of k_{cat}/K_M indicates that His12 has a pKa of 5.22 and His119 a pKa of 6.78 in the free enzyme. The pH dependence of k_{cat} shows that these are perturbed to pKa values of 6.3 and 8.1 in the enzyme-substrate complex (34).

It is generally accepted that in the cyclization step, His12 acts as a Bronsted-base catalyst to activate the 2'-OH of the ribose ring for attack (Figure 9). In the classical mechanism, His119 acts as a Bronsted acid to protonate the leaving group (Figure 9). It has also been suggested that His119 could protonate a phosphorane-like transition state (37) although

intermediate the roles of His12 and His119 are reversed. His119 activates the attack of water by Bronsted-base catalysis and His12 protonates the leaving group. It is expected from the principle of microscopic reversibility that a group reacting as a general acid in one direction will react as a general base in the opposite direction (35).

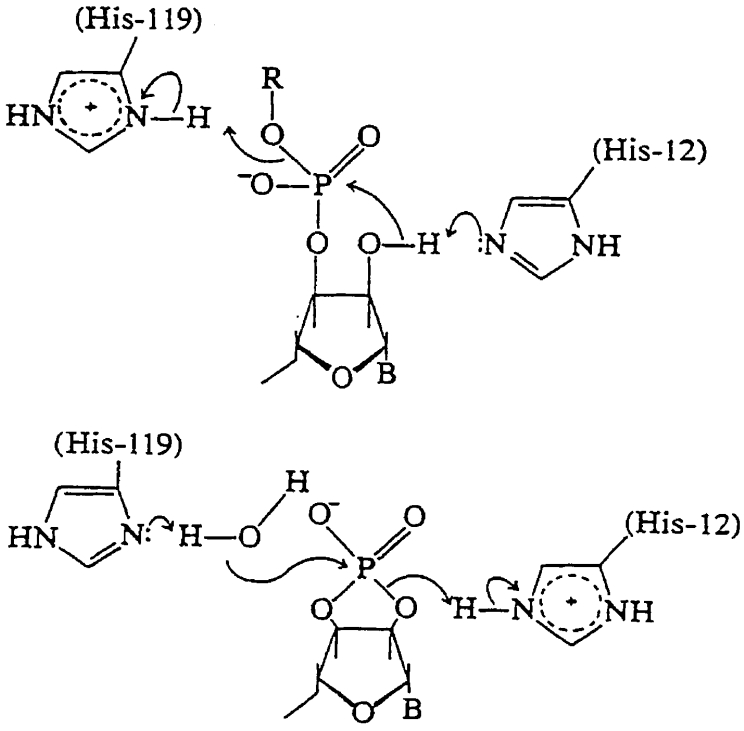

Figure 9 Mechanism of RNA hydrolysis (35)

Extensive crystallographic studies have helped to characterize the ribonuclease structure and substrate-interaction in detail (31, 32). Figure 10 shows a diagram of RNAse complexed with dATAA (shown in yellow). The enzyme binds ribonucleotides and deoxyribonucleotides equally well but only ribonucleotides are cleaved because a 2'-OH is necessary for the catalytic mechanism (39). RNAse A in fact destabilizes double-stranded DNA, i.e. it lowers the temperature of the double-helix-to-coil melting transition. This property results from its preferential binding to the single-stranded polynucleotide chain. DNA is a good inhibitor of RNAse activity and it is hypothesized that, given the similarity in the structures, complexes with DNA are representative of the RNA-protein complexes that occur during catalysis. Protein secondary structure elements (helices and sheets) are indicated by ribbons (Figure 10). The active site residues His12, His119, and Lys41 are coloured blue and the pyrimidine binding site (B_1 site-see below, Asn44, Thr45, Phe120) is coloured magenta. The His119, His12 and Lys41 side chains interact with the phosphate group of the substrate analogue, and His12 is in a position to interact the 2'-OH group of the substrate. Crystallographic studies suggested the existence of hydrogen bonds between the pyrimidine base and Thr45, Asn44, and van der waals contacts with the side chain of Phe120 (40).

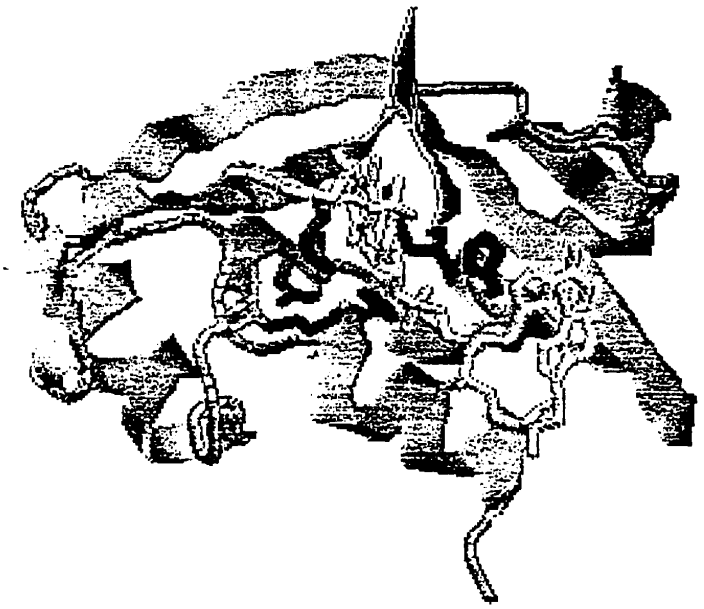

Interactions exist between RNA and substrates beyond those directly responsible for catalysis. Jensen and von Hippel (41) showed that the enzyme protected segments of single-stranded DNA 10–12 nucleotides in length. Chemical modification experiments demonstrated that several lysine and arginine residues were primarily responsible for this binding interaction. Support for the existence of multiple subsites in ribonuclease A was provided by the crystallographic analysis of complexes between the protein and tetradeoxyadenylic acid, dAAAA (32). It was found that four dAAAA molecules were partially bound to a single protein molecule. These nucleotides were observed to form a near-continuous single strand of DNA running through the active site, and over the surface of the protein. The binding between protein and nucleic acid is mainly an extended cation-anion interaction. Salt bridges are formed between phosphate groups and nine positively-charged side chains. The only important interactions involving the bases occur at the active site (39). The lysine and arginine groups are spatially complementary to the arrangement of phosphate groups along the course of a polynucleotide chain. The RNAse A structure can thus guide the single-stranded nucleic acid molecule through the active site cleft in an energy-efficient manner that does not perturb the natural conformational preferences of DNA (and RNA) (39).

Figure 11 shows a two dimensional representation of all known interactions as summarized by Pares et al.(40). The abbreviations **B**, **R**, and **p** refer to subsites involved in binding base, ribose, and phosphate respectively. The active centre subsites are responsible for the substrate specificity. The B_1 site confers a practically absolute specificity for pyrimidines (42). The B_2 subsite exhibits a preference for purines (43). Higher k_{cat} values have been reported for substrates with a purine in the 5' side of the phosphodiester bond. This activation may occur through a conformational change induced by the binding at B_2 (43).

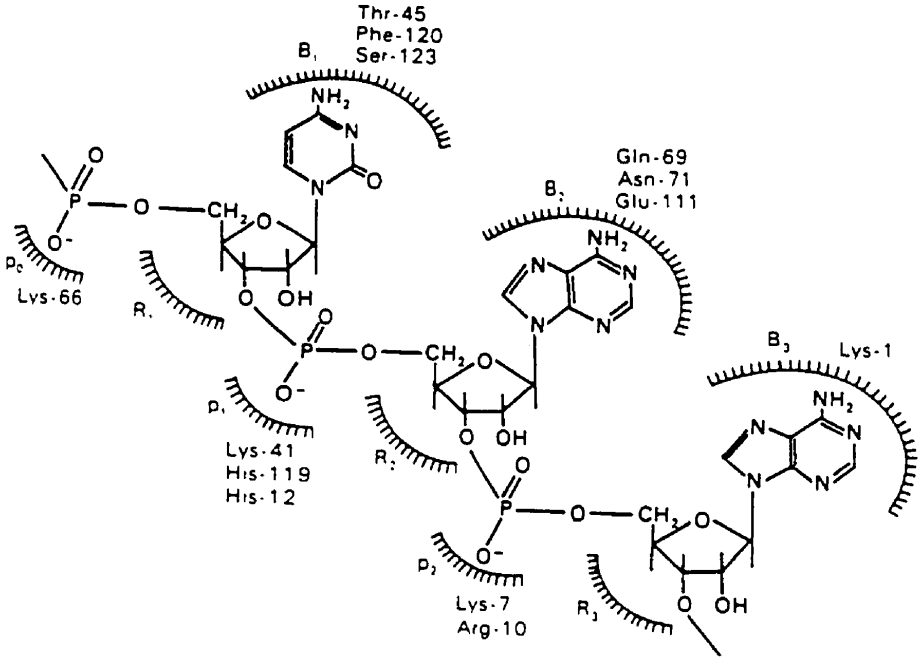

Figure 11 Schematic diagram of the active center cleft in the ribonuclease A-substrate complex (40)

Activity towards oligonucleotides increases with the chain length of the substrate (44). Experiments with oligouridylic acids of increasing chain length up to five nucleotides indicate that the kinetic parameters are almost the same for substrates with three or more nucleotide units, suggesting that the number of subsites important for catalysis corresponds to three nucleotides. However, k_{cat} for polyuridylic acid is 3 to 20 times higher (depending on the assay conditions) (44). It has been suggested that additional binding subsites play a role in the catalysis of long polynucleotides perhaps by inducing subtle conformational changes (44). The differences in k_{cat} may also reflect differences in the extent of non-productive binding.

Since the hydrolysis of the cyclic phosphate is generally slower than the first enzymatic step (33, 42), these intermediates can leave the enzyme active site and can be replaced by a new, long chain, substrate molecule. Subsequently, the shorter fragments will also be cleaved, and eventually the hydrolytic step occurs when most of the RNA has been cleaved in the transphosphorylation step.

D. Ribonuclease S

The bond between Ala20 and Ser21 in RNAse A can be cleaved by subtilisin (42). The sequence of 1-20 amino acid residues is called the S-

peptide and the other part (residues 21-124) is called the S-protein. The S-peptide remains attached to the S-protein by noncovalent interactions. If the two components are separated all enzymatic activity is lost. However, the parts will spontaneously re-associate when mixed and full enzymatic activity is restored (42). The reconstituted protein is termed ribonuclease S. Several X-ray and NMR studies have demonstrated that the three-dimensional structures of RNAse A and RNAse S are virtually identical (42).

The small size of the S-peptide makes full chemical synthesis possible. Many studies have examined the role of individual amino acids in the S peptide sequence. Hofman, Scoffone and their co-workers synthesized S-peptide and several derivatives (45, 46). S-peptide derivatives that have strong binding constants will show maximum activity at about 1:1 molar ratio to S-protein. Those S-peptide derivatives with weak binding constants require higher molar ratios for full complex formation. As mentioned above, His12 plays an important role in enzyme activity as it is involved in the enzymatic catalytic mechanism. It cannot be changed (45, 46). Semisynthetic and enzyme kinetic studies indicated that replacement of Gln11 by Glu does not influence the activity much (42). Phe8 and Met13 have a large effect on the binding affinity and help to stablize the ribonuclease S complex. Many substitutions at position 8 or position 13 affect the affinity of S-peptide for S-protein. If Phe8 and

Met13 are in the right positions for complex stabilization and His12 is also present, S-peptide will provide a productive binding to S-protein and the ribonuclease S complex will adopt a stable α-helix (47). In addition to Phe8, His12 and Met13, the incorporation of residues Glu2 and Arg10 provides an ionic interaction for stabilizing the α-helix (47). Lys7 contributes to the cationic environment of the active site (48).

Chemical synthesis of S-peptide analogues provides a convenient means for introducing non-natural amino acids since chemical synthesis of short peptides is relatively routine using solid phase synthetic techniques. Therefore we decided to use the ribonuclease S system to site-specifically incorporate the photoisomerizable residue phenylazo-phenylalanine (Pap). Since the S-peptide contributes about half of the active site cleft, this provides a direct way of incorporating photosensitive groups at site that are likely to affect enzyme activity.

EXPERIMENTAL

A. Materials and Equipment

Reagents, solvents and chemicals were purchased from Sigma Chemical Company, Aldrich Chemical Company and Caledon Laboratories Ltd. Silica gel (Merck, grade 9385, 230-400 mesh, 60A) was used for column chromatography purification of compounds. Thin Layer Chromatography (TLC) plates with silica gel (Kieselgel 60F) of 0.2 mm on aluminium from Aldrich Chemical Company were used to monitor the reactions. High Performance Liquid Chromatography (HPLC, Perkin Elmer Liquid Chromatograph with a model 250 Binary LC pump and a model LC290 UV/Vis spectrophotometric detector) was performed for purification of synthetic peptides. Perkin Elmer Unity 400 MHz ^{1}H-NMR spectroscopy, Fast Atomic Bombardment Mass Spectrometry (Fisons 70-250S mass spectrometer) and Electron Spray Mass Spectrometry were used for identification of compounds and synthetic peptides. UV/Vis spectrometer (Perkin Elmer Lamda 2) was used for the enzyme assay. MacintoshQuadra 650 and Power PC 7100 computers from Apple Computer Inc. were used for the enzyme assay and data analysis (Uvwinlab, Grafit and Igor Pro).

Peptide Synthesizer: Coupler 250 (Model # 250, Biochemical Products Dept., Du Pont Company Wilmington, DE, USA).

B. Synthesis

The synthetic route for the synthesis of Fmoc-protected phenylazophenylalnine is outlined below:

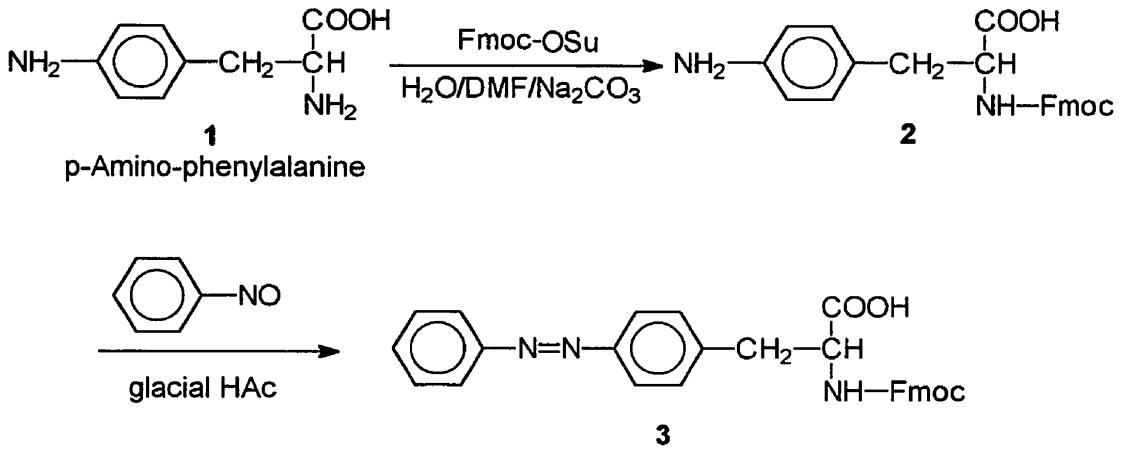

(i) Preparation of αN-Fmoc-(p-amino)-Phenylalanine

500 mg (2.22mmol) p-Amino-Phenylanaline was dissolved in 10 ml 9% Na_2CO_3 and cooled in an ice bath. A solution of Fmoc-OSu (750 mg, 2.22 mmol) in 6 ml DMF was added dropwise at 0 °C. The solution was stirred at room temperature overnight. The reaction mixture was then

diluted with 100 ml water, and extracted with ether (10 ml) and ethyl acetate (20 ml) several times to remove excess Fmoc-OSu completely. The remaining aqueous phase was acidified to pH 4-4.5 with concentrated hydrochloric acid. A white product precipitated and was then extracted with ethyl acetate (6 x 20 ml). The extract was washed with water (pH 4.5-5), dried with sodium sulphate, and the volume was reduced using a rotary evaporator. On addition of petroleum ether a white product precipitated and was collected by filtration (446 mg, yield 50%). TLC: 1-butanol:AcOH:H_2O = 2:1:1, R_f = 0.6. ^{1}H-NMR (see Appendix 1) (400MHz, in CH_3COOH-d_4): δ 3.26 ppm (q, $1H_a$, -C**H**$_2$-Ph-NH_2); δ 3.04 ppm (q, $1H_b$, -C**H**$_2$-Ph-NH_2); δ 4.18 ppm (t, 1H, -C**H**-CH_2-O-), δ 4.36-4.44 ppm (m, 2H, -C**H**$_2$-O-), δ 4.66 pmm (q, 1H, -C**H**-COOH), δ 7.30 ppm (d, $2H_a$, -Ph-**H**), δ 7.76 ppm (d, $2H_b$, -Ph-**H**), δ 7.31-7.40 ppm (m, 6H, Fmoc-**H**), δ 7.57-7.61 ppm (m, 2H, Fmoc-**H**); MS spectrum (FAB+): 403 MH^+ $C_{24}H_{23}N_2O_4$, Calc. M.W.: 403.461, Exact Mass: 403.165, High resolution found: 403.163 (see Appendix 2).

(ii) Preparation of Phenylazophenylalanine

250 mg (0.622 mmol) Fmoc-(p-Amino)-Phenylanaline was dissolved in a solution of 40 ml methanol and 2 ml glacial acetic acid, and 90 mg (1.5 eq.) nitrosobenzene was added. The reaction mixture was stirred at 70 °C for 30 hr. TLC: ethyl acetate : petroleum : methanol = 3 : 2 : 2.8, R_f =

0.4. The reaction mixture was added to water to get a precipitate, and then purified by column chromatography eluting with a solution of ethyl acetate/petroleum/methanol (3 : 2 : 2.8). The orange colour product (185 mg, yield 60.6%) was collected. UV/vis: Trans: λ_{max} = 324.93 nm, λ_{max} = 299.07 nm (small peak), λ_{max} = 289.16 nm (shoulder), λ_{max} = 264.37 nm, λ_{max} = 254.48 nm (shoulder); Cis (after irradiation): λ_{max} = 299.07 nm (small peak), λ_{max} = 287.92 nm (small peak), λ_{max} = 264.37 nm(shoulder), λ_{max} = 254.48 nm; ^{1}H-NMR (see Appendix 3) (400MHz, in CH_3COOH-d_4): δ 3.11 ppm (q,1H_a, -C**H**$_2$-Ph-), δ 3.35 ppm (q, 1H_b, -C**H**$_2$-Ph-), δ 4.17 ppm (t, 1H, -C**H**-CH_2-O-), δ 4.34-4.48 ppm (m, 2H, -C**H**$_2$-O-), δ 4.76 ppm (q, 1H, -C**H**-COOH), δ 7.21-7.42 ppm (m, 6H, Fmoc-**H**), δ 7.47-7.58 ppm (m, 5H, -Ph), δ 7.72-7.78 (m, 2H, Fmoc-**H**), δ 7.85 ppm (d, 2H_a, -Ph-**H**), δ 7.90 ppm (d, 2H_b, -Ph-**H**); MS (FAB+): MH^+ $C_{30}H_{26}N_3O_4$, M.W.: Calc. 492.5586, Exact Mass: 492.1923, high resolution found 492.1928 (see Appendix 4).

C. Peptide Synthesis

We used an automated peptide synthesizer to make the following peptide sequences:

Native peptide sequence:

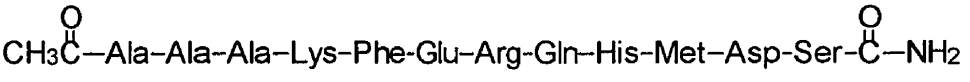

PAP-11 peptide sequence:

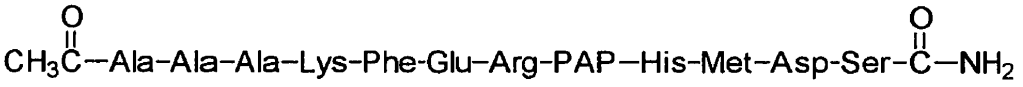

PAP-8 peptide sequence:

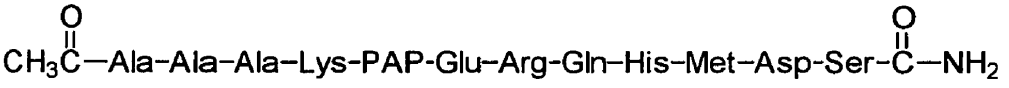

PAP-4 peptide sequence:

The Fmoc-based approach was employed (49). Initially, Pal-resin 90 mg (0.05 mmol, capacity 0.55mmol/g, Advanced ChemTech, Louisville, KY) was soaked in 25ml DMF for 1 hr and the DMF removed. Deprotection of the resin was performed by using 20% piperidine /DMF for 10-15 min. A positive result was obtained by Kaiser Test. The resin was then washed with DMF several times. Stepwise synthesis employed Fmoc-protected amino acid (3 eq. Fmoc-AA, single coupling 1-2 hr.), 3 equivalent of the coupling reagent HATU [O-(7-Azobenzotriaol-1-yl)-1,1,3,3-tetramethyluronium hexafluorophosphate], 57 mg (PerSeptive Biosystems Inc., Cat. No. GEN076521), 6 equivalent of DIPEA (N,N-

Diisopropylethylamine), 52.26 μl (Aldrich Chemical Company, Inc., Milwaukee, WI), and 15 ml NMP (N-methyl-2-pyrolidone). The Fmoc-protecting groups were removed with 20% piperidine/DMF for 15-30 min. at each step. The peptide resin was washed with NMP, then the final N-terminal acetylation was achieved with a mixture of 1.2 ml 0.5 M acetic anhydride, 1.0 ml 0.5 M pyridine and 22.8 ml NMP (total volume 25 ml) for 30 min. After acetylation, the peptide resin was washed with DMF. Cleavage of the peptide from the resin was accomplished with a 5 ml cleavage solution of 87.5% TFA, 5% water, 5% thioanisole and 2.5% EDT (1,2-ethanedithiol) votexed for at least 2 hr. The resin was rinsed with 500 ml TFA and filtered off. The cleavage cocktail was then added to 40 ml cold ether to precipitate peptide products. The peptides were dissolved in water and purified by preparative HPLC (Zorbax SB-C_{18} column 9.4 X 250 mm, eluent A, 0.1% TFA in acetonitrile, eluent B, 0.1% TFA in water, 5 - 95% eluent A gradient in 90 min., λ = 230 nm, flow rate = 2 ml/min, paper speed = 2 min/cm, AUFS: 0.1—1) and analyzed by HPLC and ES-MS. The purity by HPLC > 95%. The retention time: Native peptide, 28 min. (5 - 50% eluent A gradient in 90 min.); PAP-11, 37 min. (5 - 80% eluent A gradient in 90 min.); PAP-8, 32 min. (5 - 90% eluent A gradient in 90 min.), PAP-4, 33 min. (5 - 50% eluent A gradient in 50 min.). Mass spectra (E.S.) confirmed the products. Native peptide: calc. 1431.5, MH^+ found: 1430, PAP-11: calc.

1554.66, MH^+ found: 1554, PAP-8: calc. 1536.7, MH^+ found: 1535.6, PAP-4: calc. 1611.8, MH^+ found: 1610.8 (see Appendix 5-8).

D. Enzyme Assays

(i) CMP assay: Initially the rate of hydrolysis of cytidine 2':3' - phosphate was used to assay ribonuclease activity. In a 1 ml cuvette were mixed: 970 µl tris buffer (0.1 M, pH 7.11) + 30 µl CMP (0.1 µg/µl) + 10 µl S-protein (7 µg/µl). To this was added different amounts of native peptide solution (10 µg/µl), and the rate of change of absorbance at 280 nm was recorded. Slope (enzyme activity measured by the change of absorbance in 2 min) vs peptide concentration added was plotted.

(ii) UV/Vis assay of RNA hydrlysis (Kunitz method) (50)**:** Total yeast RNA was used as a substrate. Different amounts of S-peptide (Native peptide or PAP-peptide) were added to a constant concentration of S-protein in Na acetate buffer (0.1 M, pH 5). The rate of change of absorbance at 300 nm was recorded. Slope (enzyme activity measured by the change of absorbance in 0.2 min) vs peptide concentration added was plotted. 0.1 M (4.1015 g/500 ml H_2O) sodium acetate buffer pH 5; Substrate RNA solution: 10 µg/µl (20 mg/2 ml H_2O) RNA [purified from Torula Yeast (Sigma grade) by dialysis]; 0.052 mM (1.2 mg/2 ml H_2O) Ribonuclease S-protein (Sigma Grade XII-PR: From Bovine Pancreas). In

1 ml cuvette: 940 µl Na acetate buffer + 50 µl RNA solution + 10 µl S-protein solution

(iii) RNase Gel assay: The EnzChek™ RNase Gel Assay Kit from Molecular Probes was used. The assay was performed as described in the technical bulletin accompanying the kit: Substrate RNA 1 µl (50 ng/µl); RNase A 1 µl (2 ng/µl H_2O) (Sigma grade, type I-AS: From Bovine Pancreas; Ribonuclease S-protein 1 µl (2 ng/µl H_2O) (Sigma Grade XII-PR: From Bovine Pancreas); Native and 3 trans PAP peptides (22.4 ng/µl) with RNase-free water.

E. Photoisomerization

Photoisomerization of PAP containing peptides from the trans to cis form was accomplished using a nitrogen laser (337 nm, 150 mJ/pulse, 1.5 ns/pulse, 15 Hz pulse rate) for 15-30 minutes. The reverse isomerization (cis to trans) was accomplished by exposing the peptide solutions to diffuse sunlight a few minutes.

RESULTS AND DISCUSSION

A. Synthesis of the Photoisomerizable Amino Acid

An azobenzene containing amino acid was chosen as our synthetic target since the photochemistry of azobenzene is well-established (1) and the chromophore undergoes a large conformational change upon photoisomerization. We felt that the larger the conformational change the more likely there was to be an effect on enzyme function. A synthesis of the azobenzene-containing amino acid phenylazo-phenylalanine had been reported (Goodman's method) (51) shown below. *p*-Amino-phenylalanine reacts with nitrosobenzene in glacial acetic acid at 16-18 ^{o}C. We planned to then make the Fmoc-protected derivative for use in solid phase synthesis using Lapatsanis's method (52) as shown:

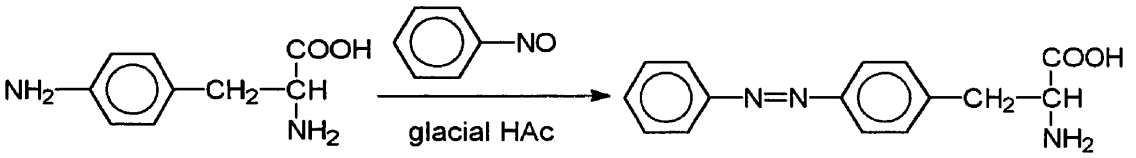

p-Amino-phenylalanine

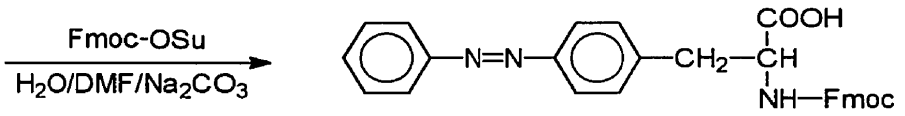

However, in our hands, the first step gave only trace amounts of product. We attributed this to reaction of the nitroso compound with the alpha amino group in competition with the amino group on the ring. Thus, we first synthesized the αN-Fmoc-(p-amino)-phenylalanine using Lapatsanis's method (52). In the workup of this reaction, several steps were found to be critical for the purity of the final product. Extensive washing the water solution with ethyl acetate and ether was necessary in order to remove Fmoc-OSu completely before the addition of acid (see experimental section). After extracting the product with ethyl acetate from the acidified water solution, again several washes were necessary to remove unreacted starting material. These two extraction steps result in pure product without the need for further purification on the column chromatography. The product is not soluble in water, chloroform or DMSO. Thus, the NMR spectrum was obtained in acetic acid CH3COOH-d_4 (Appendix 1). High resolution mass spectrometry (FAB) gave the expected mass (Appendix 2).

Goodman's method was then modified for the preparation of Fmoc-phenylazophenylalanine. Due to the insolubility of the starting material, we used methanol as solvent, with a small amount of glacial acetic acid. We found a reaction temperature of 70 ^{o}C was necessary. As the reaction proceeded the colour of reaction mixture gradually darkened until a light purple colour appeared. The mixture was then purified by

column chromatography. Most impurities, including the purple-coloured compound stayed on the top of silica gel column. After chromatography, the product was further purified by dissolving it in methanol and then adding water until precipitation occurred. The final product was also not very soluble in conventional solvents so that the NMR spectrum was obtained with acetic acid CH3COOH-d_4 (Appendix 3). High resolution FAB-MS gave the expected result (Appendix 4).

B. Synthesis and Characterization of S-Peptide Analogues

Extensive studies with S-peptide analogues have demonstrated that not the entire S-peptide (residues 1-20) is required for activity (42). A shortened analogue, comprising residues 4 to 15 is almost as active as the full S-peptide (42). We therefore synthesized a peptide with the native sequence 4-15 using standard Fmoc-based solid-phase synthesis methods (49).

Native peptide sequence:

PAP-11 peptide sequence:

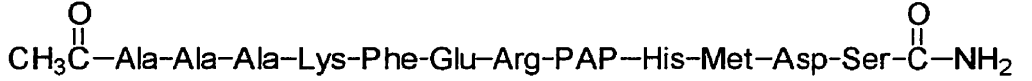

PAP-8 peptide sequence:

PAP-4 peptide sequence:

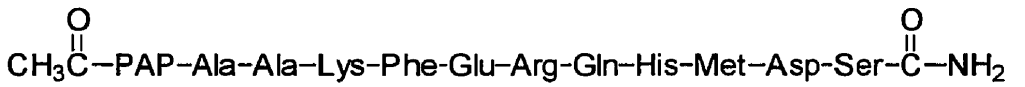

Coupling and deprotection times were found to be quite different for each Fmoc-amino acid residue in the course of the synthesis. Usually it takes an hour or two hours for coupling and twenty or thirty minutes for deprotection. However, it takes longer to finish coupling and deprotection after about the 5th residue presumably because the peptide adopts some secondary structure at this stage. As long as 5 or 6 hours was required for coupling in some cases.

Peptides were also synthesized with the phenylazo-phenylalanine residue (PAP) in positions 4, 8, and 11. These sites were chosen after examination of the three-dimensional structure of ribonuclease determined crystallographically (31, 32). We wished to choose sites that

would not interfere S-peptide binding to S-protein, but that would be likely to interfere with substrate binding or catalysis. Residue 8 does in fact contribute to the S-peptide/S-protein interaction but the naturally occurring residue at this site is Phe. We felt it might be possible for the phenylazo moiety of the PAP residue to substitute for Phe and so decided to test this position also. Residue 11 is next to His12 which is critical for the catalytic mechanism (see Introduction). Residue 4 was observed to be oriented directly into the RNA binding groove so that substitution at this site might interfere with substrate access to the enzyme.

No particular problems were encountered with either coupling or deprotection of the PAP. The native peptide was a white powder and the PAP peptides are yellow powders. All S-peptides were purified by HPLC (Zorbax SB-C18 column 9.4 X 250 mm, A: 0.1% TFA in acetonitrile, B; 0.1% TFA in water, gradient of 5 - 95% A in 90 min.) using different gradients according to the polarity of the individual peptide, and had different retention times. They were all analyzed by HPLC and ESI-MS. The purity by HPLC > 95%. All peptides had the expected mass (Appendices 5-8).

C. Photoisomerization of PAP-Peptides

Reversible trans to cis isomerization of all the PAP-containing peptides proceeded without difficulty. UV/Vis spectra were obtained for each peptide showing characteristic cis and trans-azobenzene absorption bands. Spectra for the PAP-11 peptide are shown in Figure 12. Virtually complete recovery of the trans form is observed after exposing the peptide solution to diffuse sunlight for 1-2 minutes (Figure 12). Very similar spectra were obtained for the PAP-4 and PAP-8 peptides (not shown).

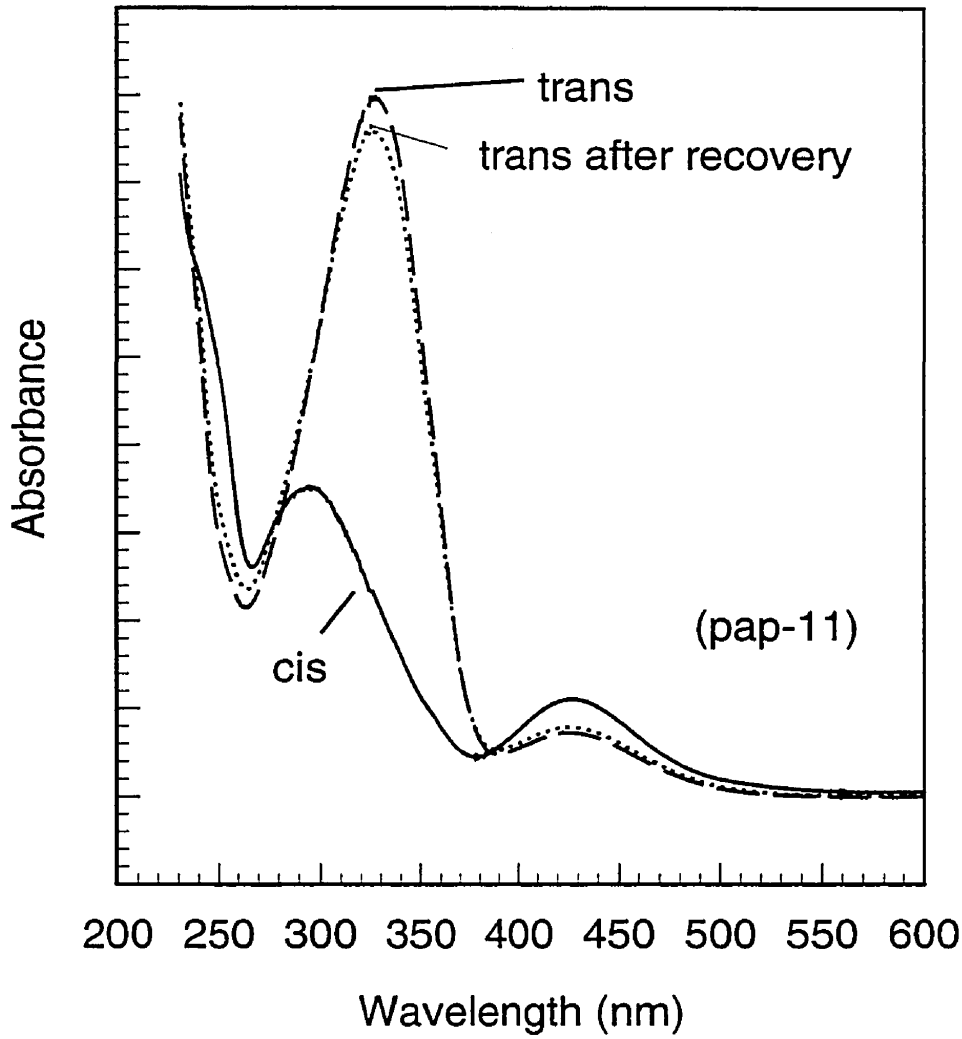

Figure 12 Reversible photochromic behaviour of the Pap-11 peptide in aqueous solution.

As is the case with most azobenzenes, the trans form is thermodynamically most stable. Nevertheless the cis-form peptides were found to be (kinetically) very stable in the dark in aqueous solution. The UV/Vis spectra were not affected by heating for at least 20hr at 25 ^{o}C, 30min at 45 ^{o}C and 30min at 60 ^{o}C.

D. Reconstitution of Enzyme Activity with Native Peptide

The ability of the native 4-15 sequence to reconstitute ribonuclease activity was assayed by measuring rates of hydrolysis of CMP (cytidine 2':3' - phosphate). Native 4-15 peptide was added to a constant concentration of S-protein in Tris buffer (pH 7.11). Figure 13 shows the rate of CMP hydrolysis as a function of the concentration of native 4-15 peptide added. Maximal activity was obtained with slightly more than a 1: 1 mole ratio of peptide to S-protein, indicating a strong association.

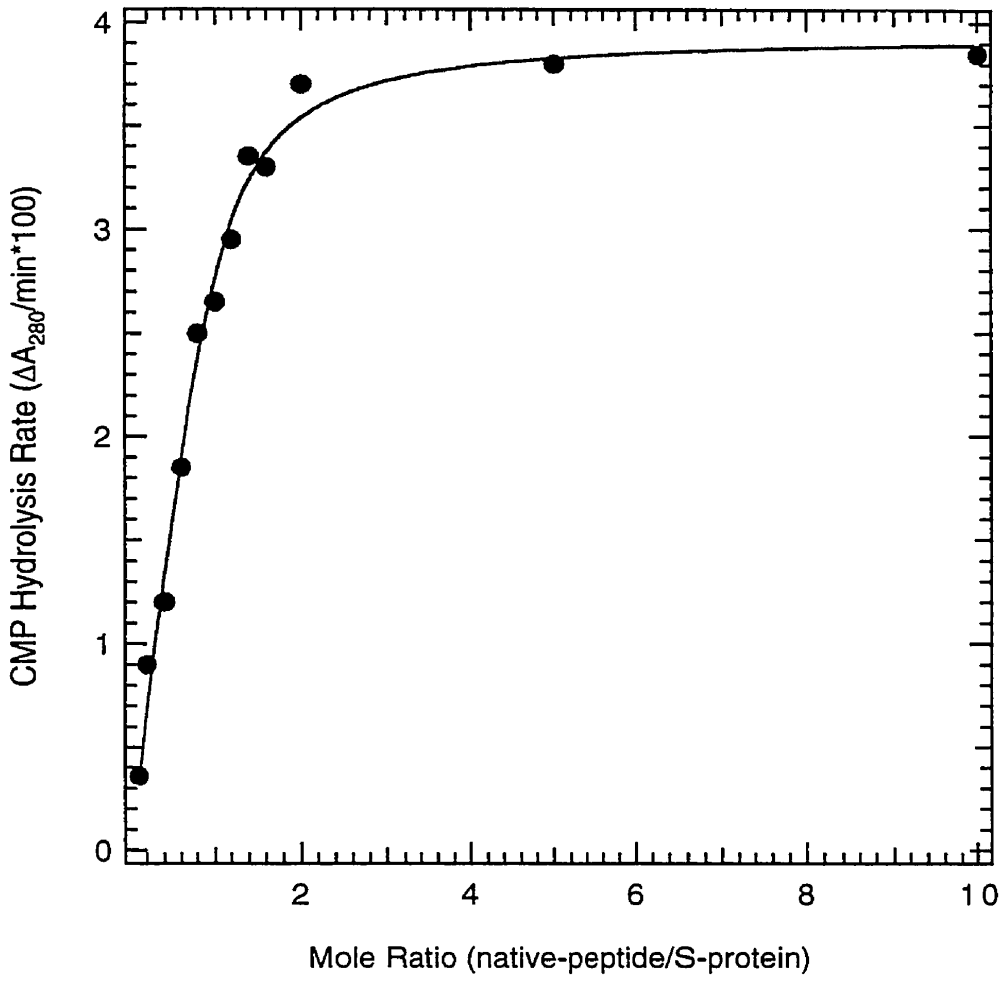

Figure 13 The rate of CMP hydrolysis vs. concentration of native peptide added.

Despite its simplicity, this assay method was judged to be unsuitable for analysis of the effects of PAP-containing peptides on enzyme activity. We do not expect simple mono- and dinucleotide substrates (42, 53) to be affected by PAP photoisomerization in the same way as RNA polymers since the conformational change (at least in the PAP-4 and PAP-8 case) is occurring at a site remote from the scissile bond. The isomerization would therefore be unlikely to have much effect on enzyme activity.

A more practical concern was that the CMP hydrolysis assay is very insensitive since the change in absorbance is small and large amounts of S protein and peptide are required. We decided to check the activity of our synthetic peptides with a commercially available gel-based assay for ribonuclease activity

E. Gel-Based Assays of Enzyme Activity

As a sensitive assay of the ability of the various S-peptide analogues to reconstitute ribonuclease activity, we employed a commercially available (Molecular Probes) gel-based kit. RNA substrate is exposed to enzyme solutions and the products applied to a standard agarose gel that separates polynucleotides on the basis of size. The molecules are visualized with an RNA stain Sybr-Green (Molecular Probes). An image of one such gel assay is shown in Figure 14 in which the activity of the

ribonuclease A is compared with S-protein complemented with native 4-15 sequence and the trans forms of PAP4, PAP8, and PAP11. The gel assay showed that trans PAP-4-RNAse S has activity similar to or slightly less than native 4-15. The trans PAP-4-RNAse S is more active than trans PAP-8-RNAse S and trans PAP-11-RNAse S. Also trans PAP-11-RNAse S is a bit more active than trans PAP-8-RNAse S. These results are consistent with those of a UV/Vis spectrophotometric assay for RNA hydrolysis (see below).

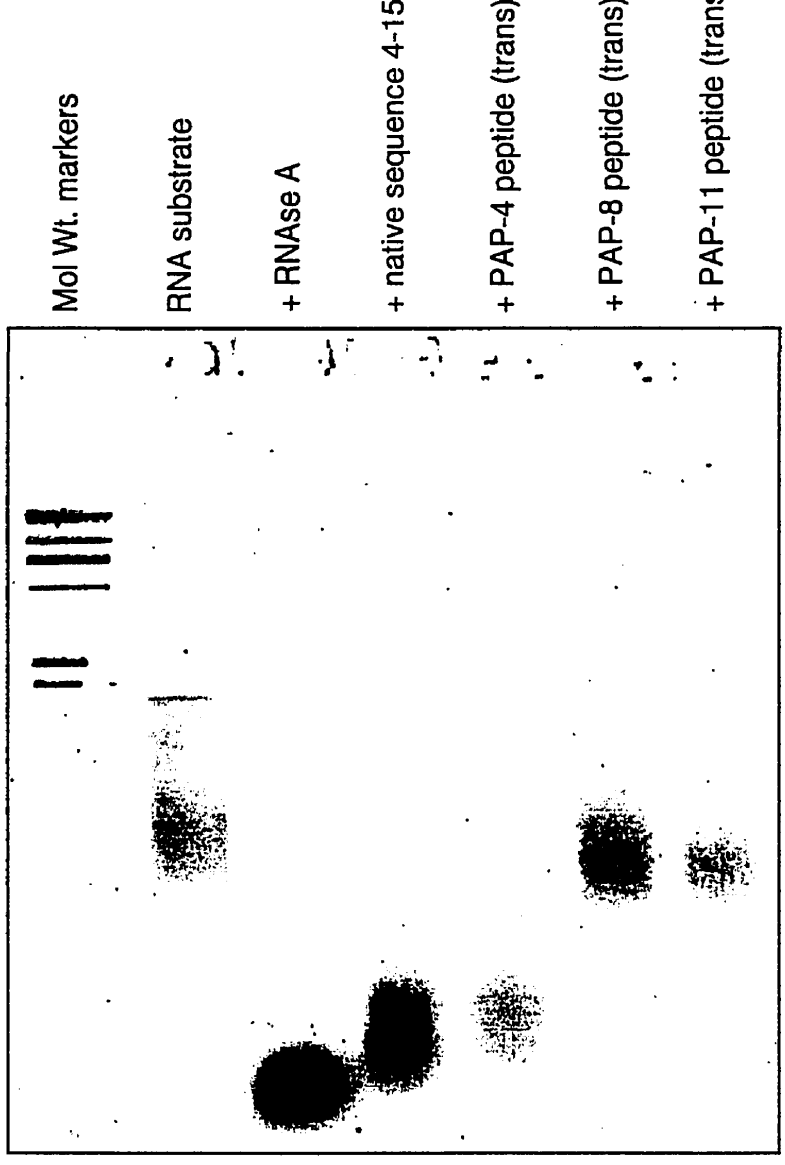

Gel Assay of Modified Ribonuclease

(per lane:50 ng RNA, 2 ng protein, 225 ng peptide)
(15 min incubation)

Figure 14

F. Effects of PAP-Peptides on Enzyme Activity

The gel-based assay gave a useful visual check for the ability of various S-peptide analogues to reconstitute ribonuclease A activity. We also attempted to use this assay to detect any differences in the activity of the PAP containing peptides upon photoisomerization. Figure 15 shows titrations of S-protein with increasing amounts of PAP-4 peptide in either cis or trans forms. Both forms of the peptide appear to be active but it is difficult to say anything conclusive about the relative activities. We therefore decided to employ another spectrophotometric assay method using total yeast RNA as a substrate. This is the classical assay developed by Kunitz (50). It too relies on small absorbance changes that occur in the substrate upon hydrolysis.

Figure 16 shows plots of initial rate of RNA hydrolysis versus concentration of peptide added to a fixed concentration of S-protein. Enzyme activity increased as peptide was added until a maximum activity was reached. This occurs when all the S-protein has bound peptide.

No ribonuclease activity was seen when excess PAP-8 peptide was added to S-protein suggesting that either a protein-peptide complex did not form or was inactive.

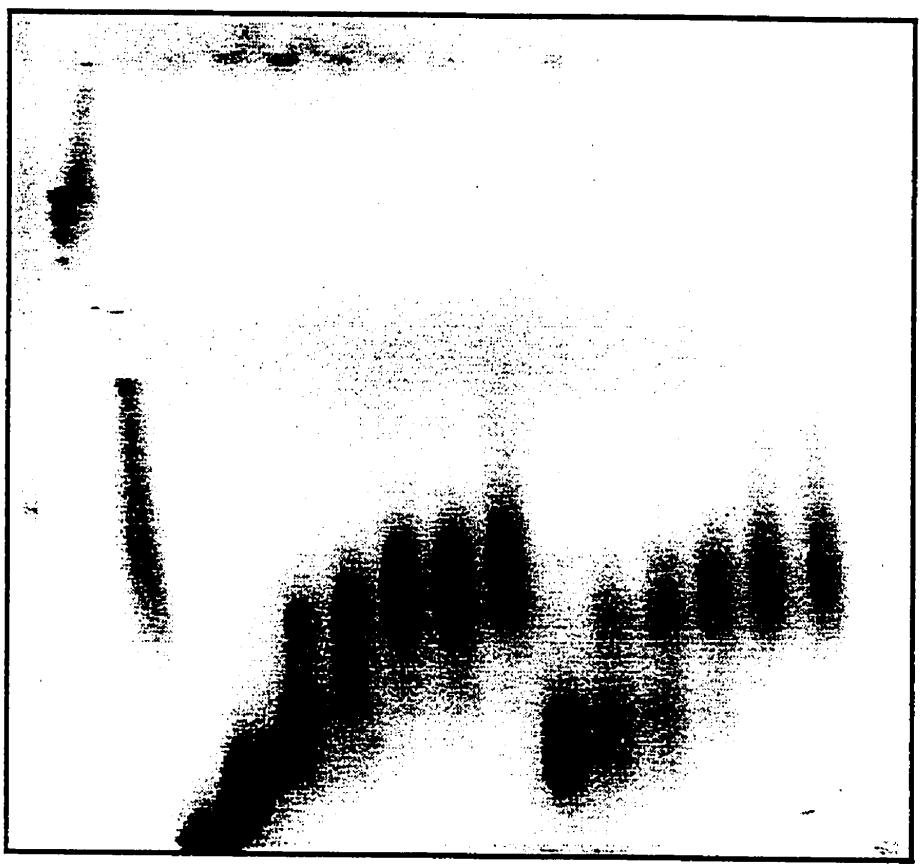

Gel Assay of Pap-4-RNase S

(per lane: 50 ng RNA, 2 ng protein)

Figure 15

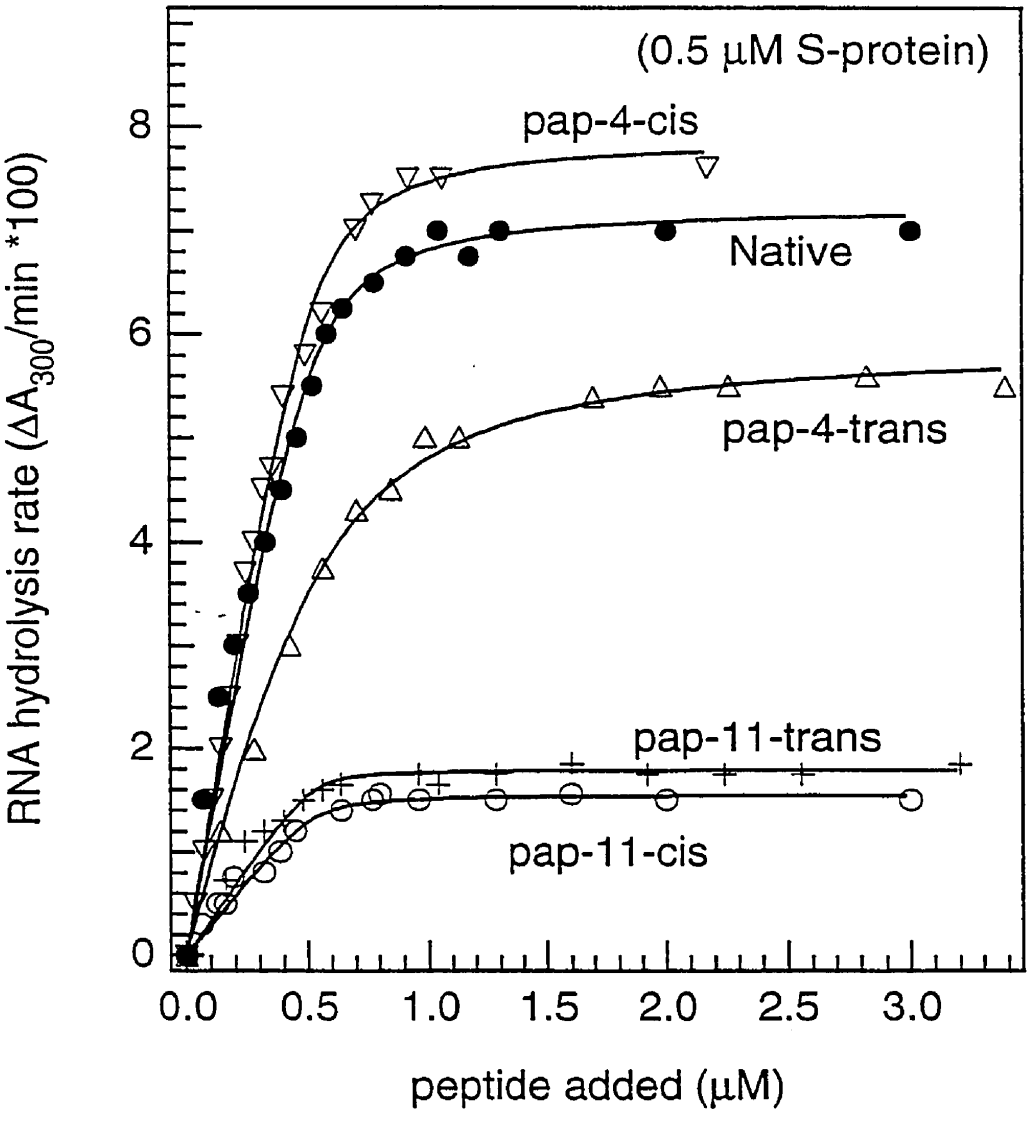

Figure 16 Hydrolysis rate vs. concentration of peptide added. (0.1 M Na acetate buffer, pH 5.0, 50 µg/mL total yeast RNA).

Thus PAP appears to be unable to substitute for Phe at this position consistent with a very well-packed structure for the native S-peptide/S-protein complex.

The PAP-11 peptide was able to restore activity to approximately the same extent in either cis or trans states. The concentration of PAP-11 peptide required for maximum activity was similar to the native case indicating that the Gln-11 to PAP-11 mutation has little effect on peptide binding to S-protein in either cis or trans forms. This is consistent with the location of this residues away from the S-peptide/S-protein interface. Both forms of the PAP-11 peptide exhibit a maximum activity about 4-fold less than that seen with the native peptide. Molecular modelling studies of PAP-11-RNAse S performed by John Karanicolas in the lab suggest that cis and trans forms of the PAP11 residue occupy similar regions of space (Figure 17). Thus any steric effect on RNA hydrolysis is likely to be the same for both isomers.

The PAP-4 cis peptide restored activity to a maximum level somewhat higher than that of the native peptide at the same concentration. The PAP-4 trans peptide, on the other hand, showed a maximum activity about 25% less than the PAP-4 cis peptide and a slightly lower affinity for the S-protein. Molecular modelling of the PAP4-RNAse S indicates the PAP residue occupies significantly different positions in space, at least in

Figure 17 Molecular surface representation of PAP-11 modified ribonuclease S. The PAP-11 cis form is coloured orange and the trans form is coloured pink. The His residues of the active site are coloured blue. The pyrimidine binding site (B1) is coloured green and the purine binding site (B2) is coloured brown.

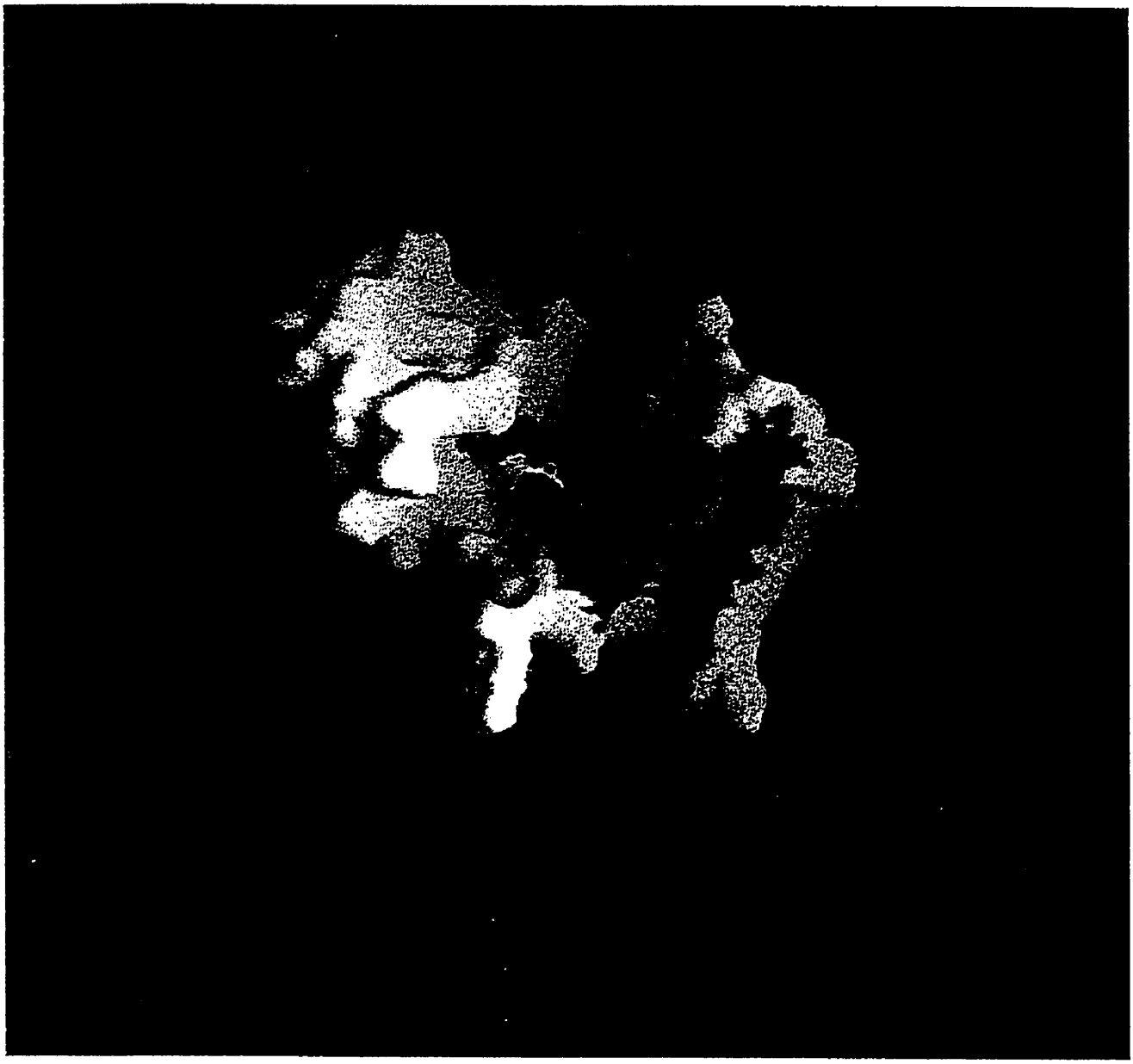

Figure 18 Molecular surface representation of PAP-4 modified ribonuclease S. The PAP-4 cis form is coloured orange and the trans form is coloured pink. The His residues of the active site are coloured blue. The pyrimidine binding site (B1) is coloured green and the purine binding site (B2) is coloured brown.

the absence of substrate (Figure 18). This difference may underlie the difference in enzyme activities seen. Unfortunately the relatively low sensitivity of the Kunitz assay makes accurate determination of Vmax and Km values of the mutant enzymes difficult. It is thus not possible at present to determine if the conformational change of PAP-4 affects binding of the substrate or if it affects the chemical step (or both).

SUMMARY AND FUTURE DIRECTIONS

This work has demonstrated the basic feasibility of incorporating photoisomerizable residues site-specifically into the active site of an enzyme. Although the observed effects of photoisomerization on enzyme activity are not large, the availability of high resolution crystal structures of free and substrate-bound ribonuclease (54) should facilitate interpretation of changes in activity upon photoisomerization (or the lack of a change as with PAP-11) in terms of the structure and dynamics of the modified protein.

Future work must include the development of better polymeric substrates so that a full kinetic analysis is possible. It will be important to know if photoisomerization is affecting Km (as expected) or kcat. The modelling studies in combination with the activity assays suggest that more substantial conformational changes will be necessary if significant changes in enzyme activity are desired. Thus bulkier analogues of PAP or other photoisomerizable amino acid analogues may be better suited for site-specific incorporation. It appears however, that the ribonuclease system, is well suited for a rational approach to the photoregulation of an enzyme.

REFERENCES

1. *Biological Applications of Photochemical Switches, Bioorganic Photochemistry Series, Volume 2,* (Eds.: Harry Morrison), Wiley, Chapter 1, 1993
2. I. Willner and S. Rubin, Angew. Chem. Int. Ed. Engl. **35**, 367-385, 1996
3. V. N. R. Pillai, *Synthesis*, **1**, 1990
4. R. W. Binkley, T. W. Flechtner in *Synthetic Organic Photochemistry* (Ed.: W. M. Horspool), Plenum, New York, p. 375, 1984
5. J. Bieth, S.M. Vratsanos, N. H. Wassermann, B. F. Erlanger, *Proc. Natl. Acad. Sci. USA,* **64**, 1103, 1969
6. J. Bieth, S.M. Vratsanos, N. H. Wassermann, B. F. Erlanger, *Proc. Natl. Acad. Sci. USA,* **66**, 850, 1970
7. K. T. Galley, M. DeSorgo, W. Prins. *Biochem. Biophys. Res. Commun.* **50**, 300, 1973
8. M. A. Wainberg, B. F. Erlanger, *Biochemistry,* **10**, 3816, 1971
9. E. Bartels, N. H. Wassermann, B. F. Erlanger, *Proc. Natl. Acad. Sci. USA,* **68**, 1820, 1971
10. P. R. Westmark, J. P. Kelly, B. D. Smith, *J. Am. Chem. Soc.* **115**, 3416, 1993
11. B. F. Erlanger, *Annu. Rev. Biochem.* **45**, 267, 1976

12. O. Pieroni, J. L. Houben, A. Fissi, P. Costantino, F. Ciardelli, *J. Am. Chem. Soc.* **102**, 5913, 1980

13. J. L. Houben, A. Fissi, D. Baccida, N. Rosato, O. Pieroni, F. Ciardelli, *Int. J. Biol. Macromol.* **5**, 94, 1983

14. F. Ciardelli, O. Pieroni, J. L. Houben, A. Fissi, *Biopolymers* **23**, 1423, 1984

15. F. B. Perler, F. S. Gimble, J. Thorner, *Nucleic Acids Res.* **22**, 1125-1127, 1994

16. F. S. Gimble, J. Thorner, *Nature* **357**, 301-306, 1992

17. B. L. Stoddard, J. Bruhnke, P. Koenigs, N. Porter, D. Ringe, G. A. Petsko, *Biochemistry* **29**, 8042-8051, 1990

18. P. G. Schultz, et al. *Science* **255**, 197-200, 1992

19. U. Zehavi, A. Patchornik, B. Amit, *J. Org. Chem.* **37**, 2281-2284, 1972

20. T. E. Creighton, *Proteins, Structures and Molecular Properties*, W. H. Freeman, New York, 1984

21. M. L. Bender, R. J. Bergeron and M. Komiyama, *The Bioorganic Chemistry of Enzymatic Catalysis*, Wiley, New York, 1984

22. P. V. Argade, G. K. Gerke, J. P. Weber, and W. L. Peticolas, *Biochemistry*, **23**, 299-304, 1984

23. A. D. Turner, S. V. Pizzo, G. W. Rozakis, N. A. Porter, *J. Am. Chem. Soc.* **109**, 1274, 1987

24. A. D. Turner, S. V. Pizzo, G. W. Rozakis, N. A. Porter, *J. Am. Chem. Soc.* **110**, 244, 1988

25. I. Willner and S. Rubin, A. Riklin, *J. Am. Chem. Soc.* **113**, 3321, 1991

26. R. Verger, M. C. E. Mieras, G. H. de Haas, *J. Biol. Chem.* **248**, 4023, 1973

27. W. A. Pieterson, J. C. Vidal, J. J. Volwerk, G. H. de Haas, *Biochemistry* **13**, 1455, 1974

28. M. C. E. van Dam-Mieras, M. C. E. A. J. Slotboom, W. A. Pieterson, G. H. de Haas, *Biochemistry* **14**, 5387, 1975

29. T. Ueda, K. Murayama, T. Yamamoto, S. Kimura, Y. Imanishi, *J. Chem. Soc. Perkin Trans.* **1**, 225, 1994.

30. C.H.W. Hirs, S. Moore and W.H. Stein, *J. Biol. Chem.* **235**, 633, 1960

31. A. McPherson, G. Brayer and R. Morrison, *J. Mol. Biol.* **189**, 305-327, 1986

32. A. McPherson, G. Brayer and R. Morrison, *Biophys J.* **49**, 209-219, 1986

33. P. Blackburn and S. Moore, *The Enzymes* **15**, 317-433, 1982

34. M.E. Eftink and R.L. Biltonen, *Hydrolytic Enzymes*, chapter 7, pp. 333-376, Elsevier Science Publishers, Amsterdam, New York and Oxford, (1987)

35. A. Fersht, 2nd edition, *Enzyme structure and mechanism*, Chapter 15, 426-428, 1985

36. C. M. Cuchillo, et al., *Biochemistry,* **26**, 89-103, 1991

37. D. M. Perreault and E. V. Anslyn, *Angew. Chem. Int. Ed. Engl.* **36**, 432-450, 1997

38. A. Fersht, 2nd edition, *Enzyme structure and mechanism*, Chapter 5, 1985

39. A. McPherson, G. Brayer, D. Cascio and R. Williams, *Science* **232**, 765-768, 1986

40. X. Pares, R. Liorens, C. Arus and C. M. Cuchillo, *Eur. J. Biochem.* **105**, 571-579, 1980

41. D. E. Jensen and P. H. von Hippel, *J. Biol. Chem.* **251**, 7198-7214, 1976

42. F. M. Richards and H. W. Wyckoff, *The Enzyme* **4**, 647-806, 1971

43. C. Arus, L. Paolillo, R. Llorens, R. Napolitano and C. M. Cuchillo, *Biochemistry* **21**, 4290-4297, 1982

44. M. Irie, F. Milkami, K. Monma, K. Ohgi, H. Watanabe, R. Yamaguchi and H. Nagase, *J. Biochem. (Tokyo)* **96**, 89-96, 1984

45. Hofman, K. and Bohn, H. *J. Am. Chem. Soc.* **89**, 5914, 1966

46. Scoffone, E. et al *JCS,C* 606, 1967

47. E. Scoffone, et al *Medicinal Chemistry III, Milan, Special Contributions,* Pratesi, P., Ed., Butterworths, London, 83, 1973

48. P. J. Vithayathil and F. M. Richards, *J. Biol. Chem.*, **135**, 1029, 1960

49. E. Atherton and R. C. Sheppard, *Solid Phase Peptide Synthesis: A practical Approach,* IRL Press: Oxford, England, 1989

50. M. Kunitz, *J. Biol. Chem.* **164**, 563, 1946

51. M. Goodman and A. Kossoy, *J. Am. Chem. Soc.* **88:21**, 5010, 1966

52. L. Lapatsanis, G. Milias and M. Kolovos, *Communications*, 671-673, August 1983

53. K. M. Postek, T. LaDue and R. K. Sandwick, *Anal. Biochem.* **203**, 47, 1992

54. J. C. Fontecilla-Camps, R. de Llorens, M. H. le Du and C. M. Cuchillo, *J. Biol. Chem.* **269**, 21526, 1994

^{1}H-NMR spectrum of αN-Fmoc-(p-amino)-Phenyalanine in CH_3COOH-d_4

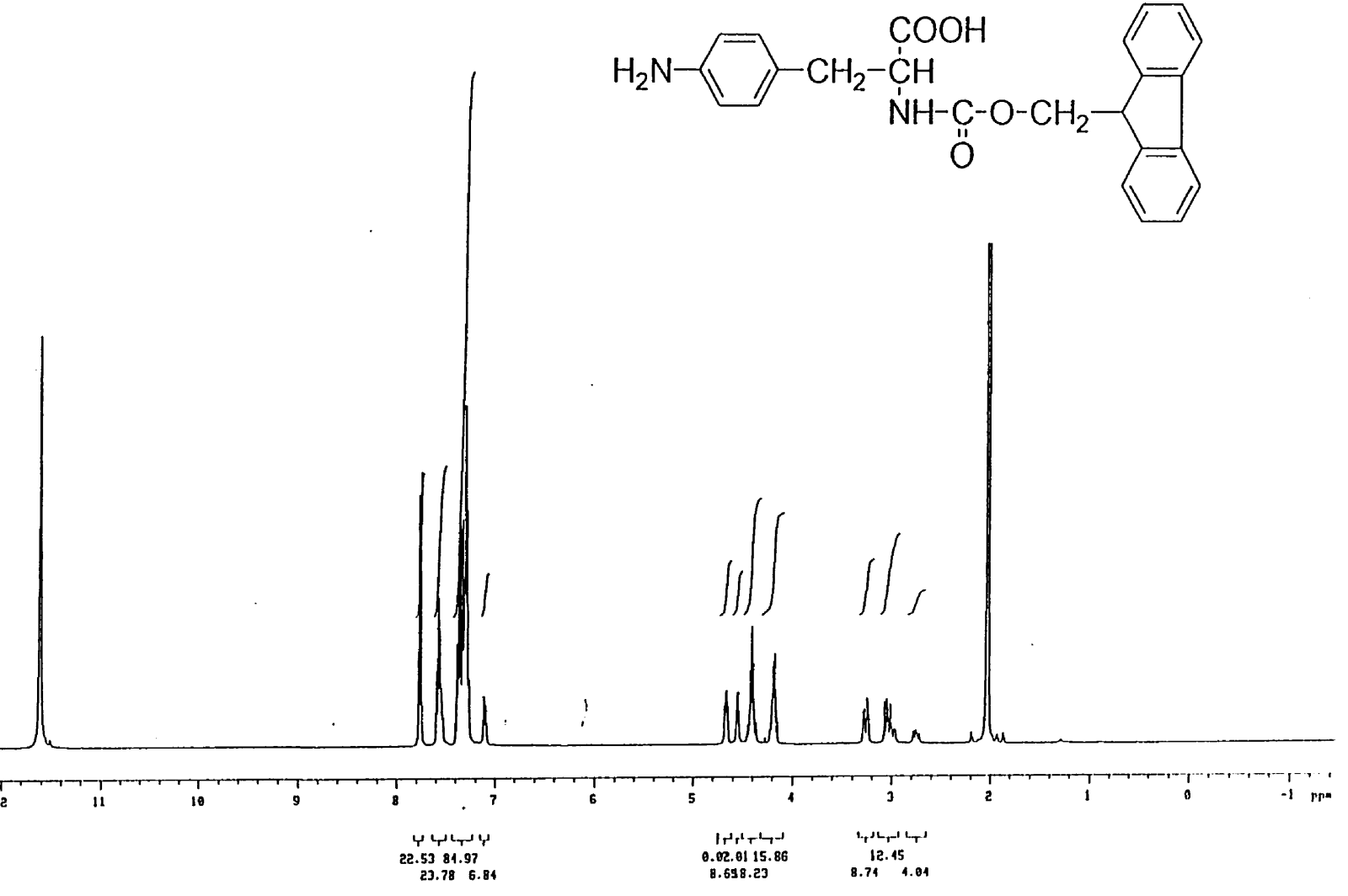

MS spectrum of αN-Fmoc-(p-amino)-Phenylalanine (FAB, High resolution, Exact mass: 403.165)

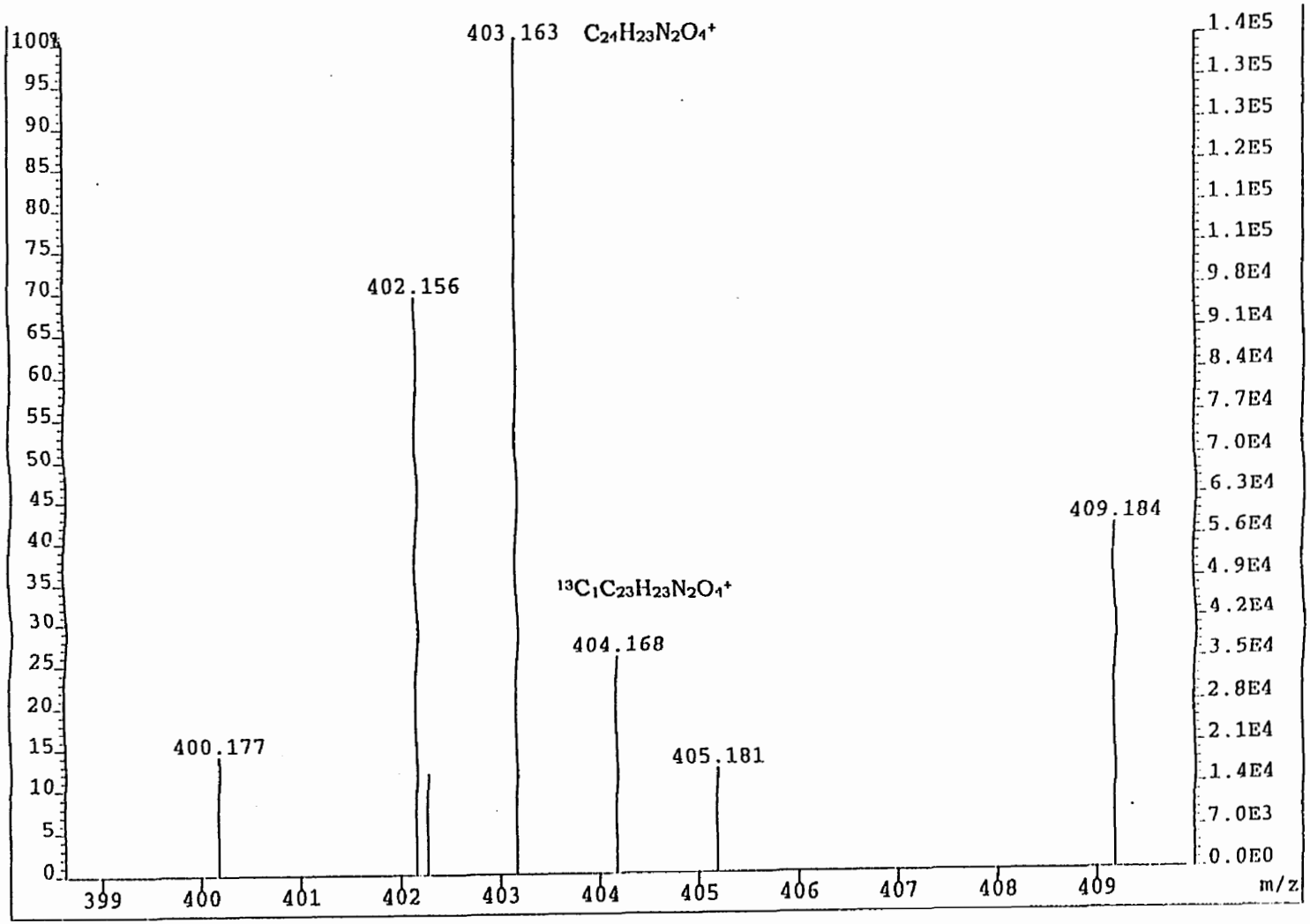

-NMR spectrum of Phenyazophenylalanine in CH_3COOH-d_4

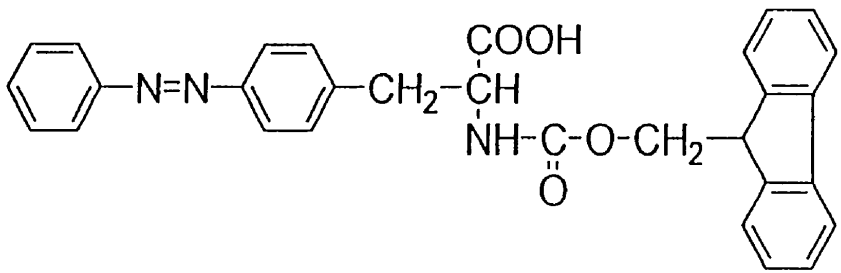

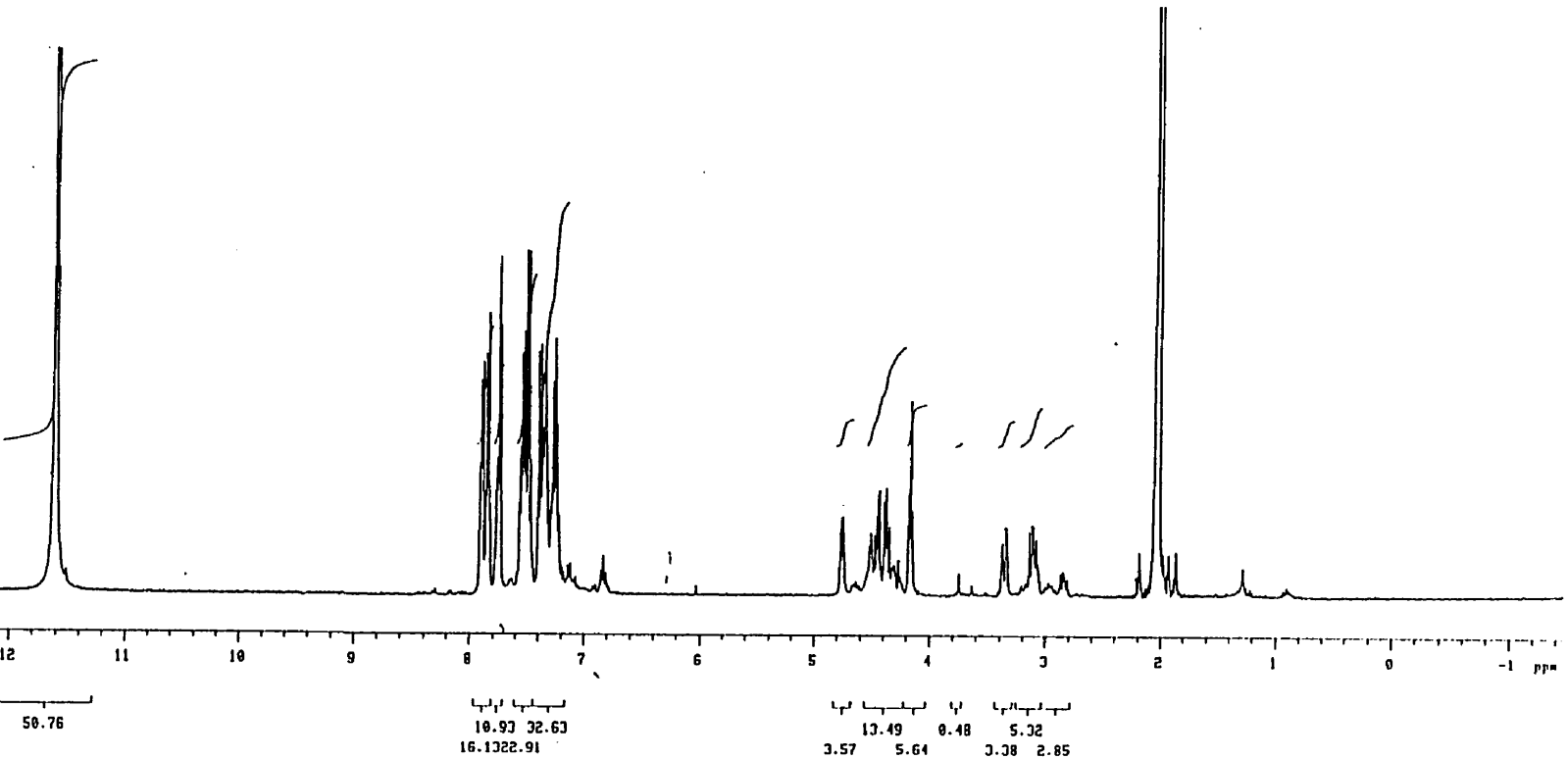

MS spectrum of Phenylazophenylalanine
(FAB, High resolution, Exact mass: 492.1923)

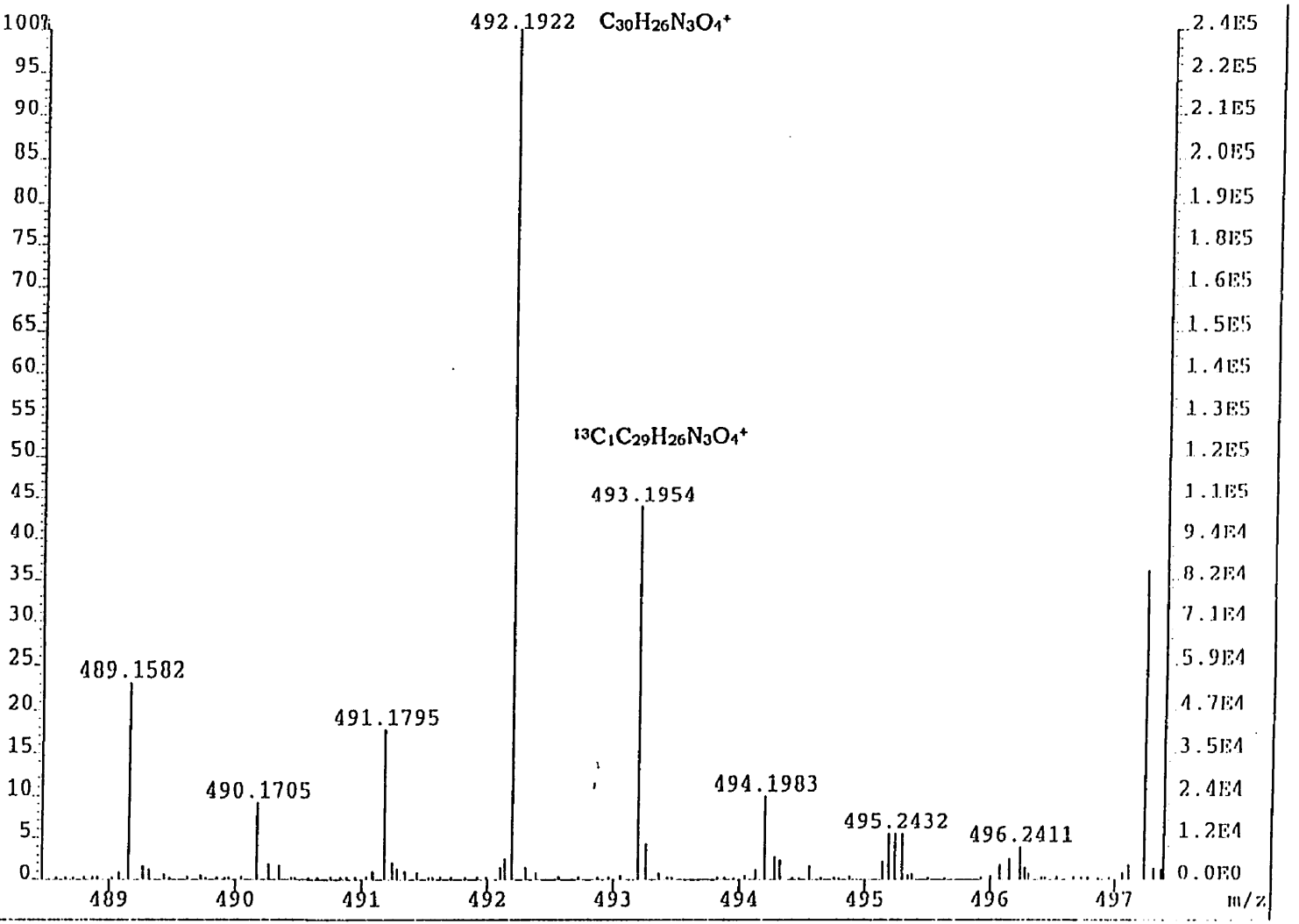

MS spectrum of Native-peptide (E.S., M.W.=1431.5)

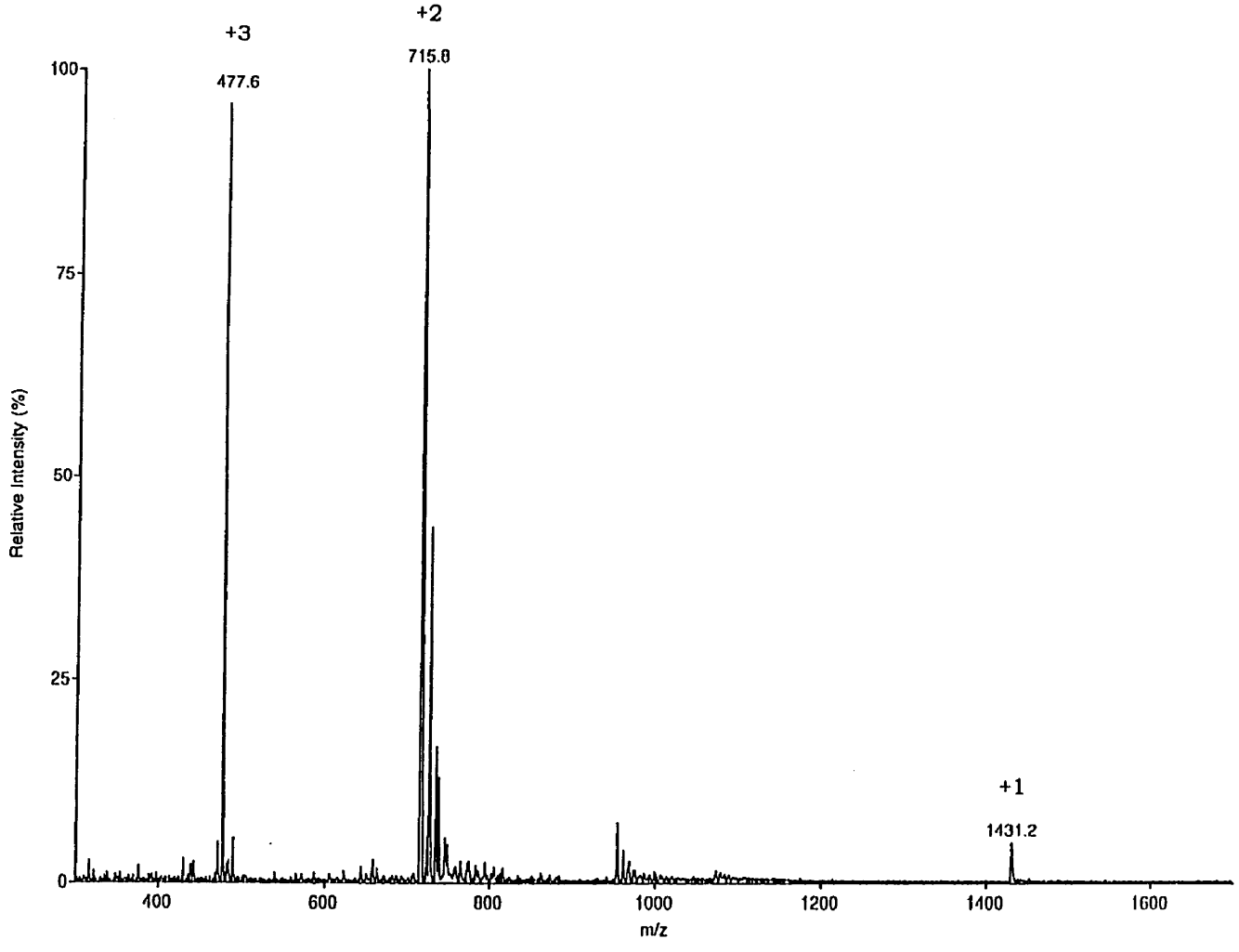

MS spectrum of Pap-11-peptide (E.S., M.W.=1554.66)

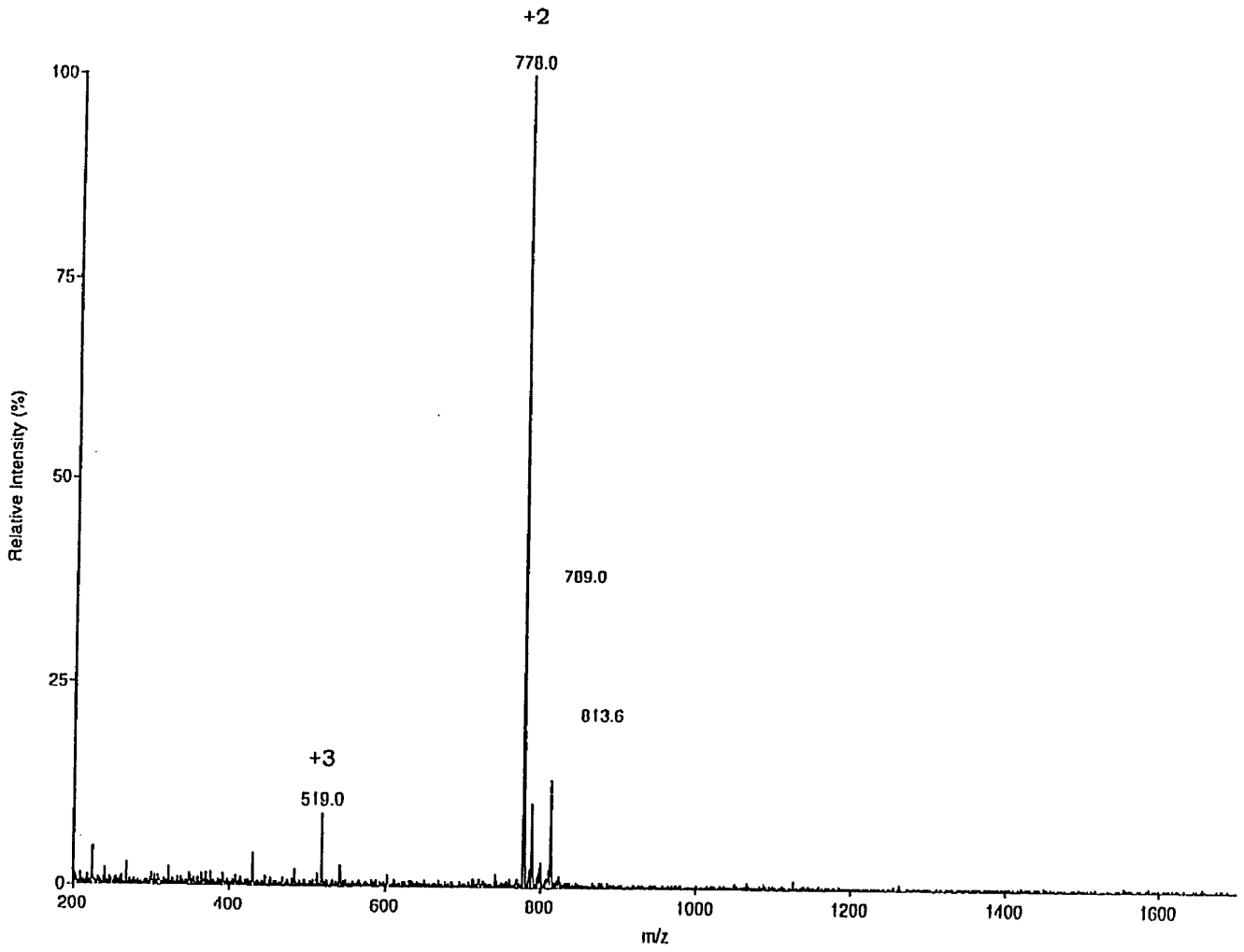

MS spectrum of Pap-8-peptide (E.S., M.W.=1536.7)

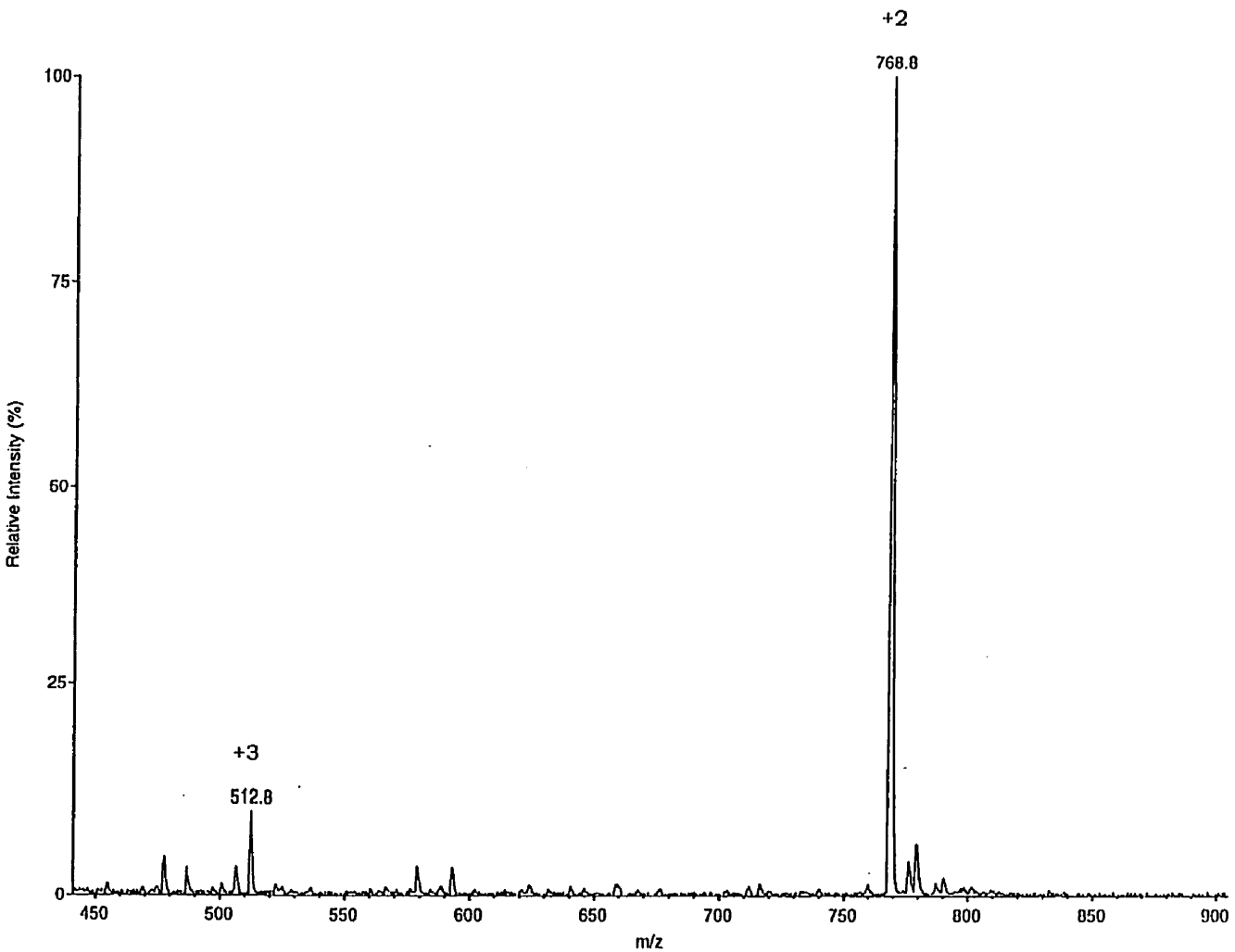

MS spectrum of Pap-4-peptide (E.S., M.W.=1611.8)

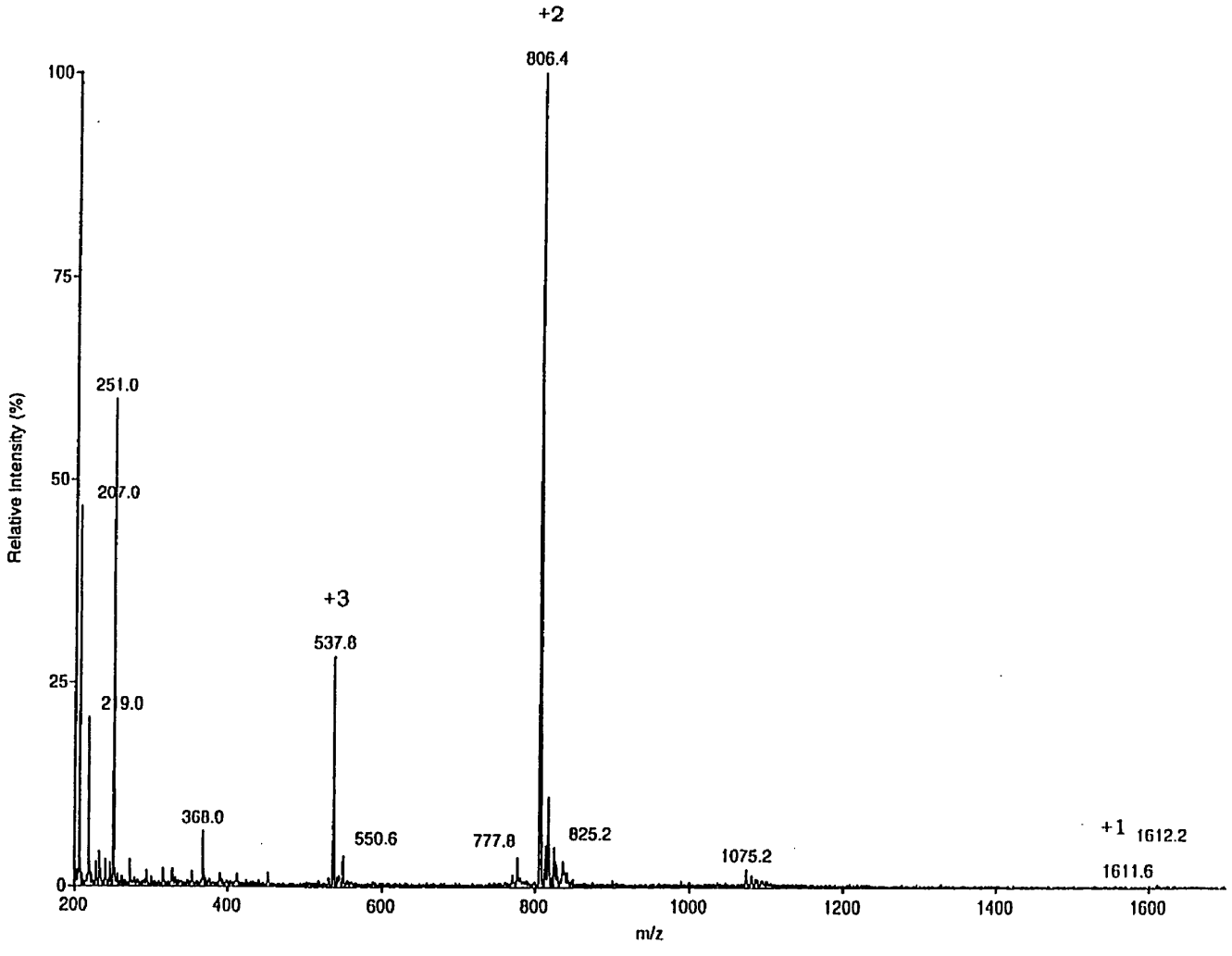

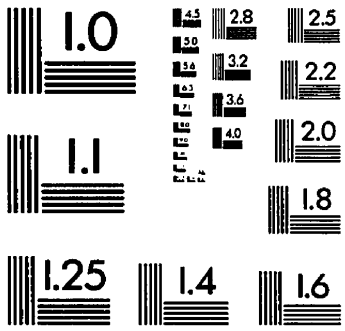

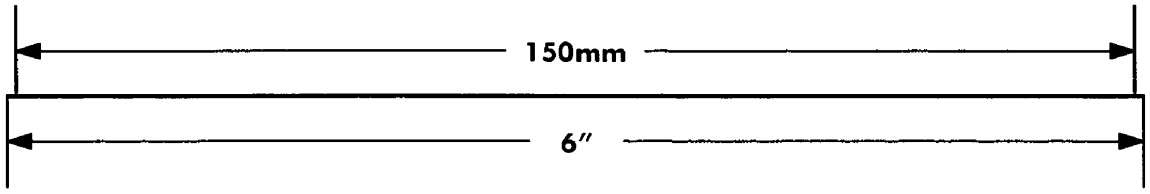

APPLIED IMAGE, Inc
1653 East Main Street
Rochester, NY 14609 USA
Phone: 716/482-0300
Fax: 716/288-5989